Impact of wind penetration in electricity markets on optimal power-to-heat capacities in a local district heating system

Hrvoje Dorotić*, Marko Ban, Tomislav Pukšec, Neven Duić

University of Zagreb, Faculty of Mechanical Engineering and Naval Architecture,

Department of Energy, Power Engineering and Environmental Engineering, Ivana Lučića 5, 10002, Zagreb, Croatia

**corresponding author, contact email: hrvoje.dorotic@fsb.hr*

Abstract

While the share of intermittent renewable energy sources in a power sector is constantly increasing, demand response technologies are becoming a crucial part of interconnected energy systems. The district heating sector has a great potential of offering such services if power-to-heat and thermal storage technologies are implemented. This is a well-known method of utilizing low-price electricity from the power market. However, power-to-heat optimal supply capacities are rarely studied with respect to different market conditions, especially from the point of view of multi-objective optimization. This paper shows an analysis of the impact of a wind production increase in a power market on optimal power-to-heat capacities in a local district heating system. To obtain these results, a district heating optimization model was developed by using linear programming, while the power market prices reduction is analysed by using historical bidding market data and shifting of the supply curve. The district heating model was created in the open-source and free programming language called Julia. The model was tested on a case study of the Nord Pool electricity market and a numerical example of a district heating system. The main outcome of this research is to show how district heating supply technologies operate in different market conditions and how they affect optimal power-to-heat and thermal storage capacities. Heat pump capacities linearly follow wind production increase in power markets.

Keywords*:* district heating, energy planning, power-to-heat, power market, multi-objective optimization

Word count: 8 800

Highlights

- The impact of wind penetration in electricity markets on the optimal results of a district heating system has been studied
- The increase of optimal heat pump capacity and heat production linearly follows wind penetration in power markets
- Optimal thermal storage size and heat pump capacity can be doubled for higher shares of wind energy in a power market

Abbreviations

DH	district heating
RES	renewable energy sources
CHP	cogeneration

Chemical formulas

CO_2	carbon dioxide

Variables and parameters

A_{ST}	area of solar thermal collectors [m^2]
a_1	first order heat loss coefficient [W/K]
a_2	second order heat loss coefficient [W/K^2]
C	cost [EUR]
DEM	district heating demand [MW]
f_{ecol}	ecological objective function (tonnes of CO_2)
f_{econ}	economical objective function (EUR)
$f_{Lorentz}$	Lorentz factor of the heat pump [-]
G	global solar radiation [W/m^2]
MCP	market clearing price [EUR/MWh]
MCP'	reduced market clearing price [EUR/MWh]
P	supply capacity [mw]
P_t	hourly market price [EUR/MWh]
Q	thermal energy [MWh]
$r_{up-down}$	ramping limit of technology [h^{-1}]
SOC	state-of-charge [MWh]
T	temperature [K]
TES	thermal storage
TES_{in-out}	thermal storage charge and discharge [MW]
V	market volume [MWh]

Greek letters

η	technology efficiency [-]
η_0	optical efficiency of solar thermal collector [-]

Scripts

D	demand
i	technology type
ref	reference
S	supply
t	time

1. Introduction

This section provides an overview of district heating systems and the power market. Additionally, different market clearing price modelling approaches are shown while focusing on the wind penetration influence. Furthermore, the latest publications dealing with district heating and power sector integration have been reviewed. Finally, the scientific contribution of this paper is presented.

1.1. District heating systems

District heating (DH) is a relatively old concept but has been widely acknowledged as one of the crucial technologies for covering future heating demand [1], [2]. The reduction of specific heating demand will result in a reduction of supply temperatures in the DH system and an increase of overall efficiency of the thermal network. This will open possibilities for the integration of low temperature heat sources and waste heat [3] combined with heat pumps [4]. Lund has defined the fourth generation of DH which is now accepted as the standard for low temperature DH which is integrated with other sectors, thus creating a so called smart energy system [5]. In smart energy systems, DH will have a crucial role by integrating the power and heat sector through power-to-heat technologies such as heat pumps or electrical heaters [5], [6]. These units are able to efficiently and effectively transform electricity into thermal energy [7], [8]. The implementation of booster heat pumps has been studied in [9], while the combination of power-to-heat technologies in the hybrid district heating system is studied also in [10]. Such integration allows a higher penetration of variable renewable energy sources (RES) such as wind or solar photovoltaics into the power sector [11]. Sayegh et al have shown the trend of the research related to DH [12], while emphasizing the importance of thermal storage technologies and integration with other sectors, thus creating a smart energy system. Besides providing a demand response for the power sector, DH will potentially have other important roles, as discussed in [13]. However, some papers have already discussed the next generation of DH and the present existing cases in Europe [14]. Ultra-low temperature district heating systems can offer additional benefits for the integration of heat pumps due to the increased coefficient of performance. Arabkoohsar and Alsagri analysed the impact of integrating heat pumps in DH systems with three pipes [15]. Although researchers are exploring power and heating sector integration, there is still a great number of coal power plants in Europe which need to be refurbished or upgraded in order to reach the standard of the 3rd generation of DH [16].

1.2. Wind integration in power systems

The power market enables the purchasing of electricity through bidding – electricity producers sell electricity, while various consumers can buy it according to the market rules. When market supply and market demand are balanced, market equilibrium is achieved. It is defined with a market clearing price and market volume. Due to their production variability on an hourly level and market readiness, wind energy production and its successful integration in power markets presents a crucial topic for numerous authors. In order to evaluate a market clearing price and conventional production optimization with a high share of wind penetration, various methods have been proposed. Paper [17] studies wind profit maximization in the day-ahead power market by using a utility function which models the behaviour of electricity customers. The main goal is to utilise demand response technologies to achieve a higher profit for wind

generation. Li and Shi adopted an agent-based simulation to analyse the bidding optimisation of wind generation in a deregulated day-ahead power market. They have shown that it is possible to increase net earnings by using learning algorithms [18]. In paper [19] different aspects of wind energy system modelling have been taken into account in order to study the integration of mentioned technologies in a deregulated power market. Reddy et al [20] proposed a novel market clearing mechanism for a wind-thermal power system while taking into account different uncertainties in production. An optimal scheduling strategy has been acquired for a best-fit day-ahead schedule. Paper [21] analysed wind penetration in interconnected regional power systems while taking into account different uncertainties. The authors showed how higher economic efficiency could be achieved by enabling cross-border trading. Fogerlber and Lazarczyk have studied the impact of wind power volatility on production failures in other production units in the power market [22]. The focus was put on Nord Pool. The issue of successful wind power integration into the power market was also studied in paper [23]. The authors analysed the effect of spatial diversification of wind power on its market value. A case study of Chile was used and the obtained results showed that spatial diversification could vary up to $10/MWh. Cuervo and Botero [24] discussed wind power reliability in a hydro-dominated power system, where Colombia was used as the case study. It was shown that higher wind penetration causes higher reservoir levels for the same hydrological conditions. This also caused the reduction of electricity market prices.

1.3. District heating and power market integration

Optimization of DH systems often includes the possibility of utilizing power-to-heat technologies such as compression heat pumps with various heat sources and electrical heaters. Single objective optimization most often includes the minimization of total cost while optimizing supply capacities and the hourly operation of supply units [25]. In research [26], single objective optimization of DH was carried out, as well as an additional analysis of the effect of feed-in tariff supporting schemes. Power-to-heat technologies are also often included in multi-objective optimization problems, where more than one objective function is defined. It should be mentioned that the result of multi-objective optimization is not a single value but a whole set of values which lie on the Pareto front. Paper [27] used genetic algorithm in order to obtain optimal supply capacities and the hourly operation of the DH system. In [28] combined heating and cooling systems were studied in order to obtain optimal capacities of electric and absorption chillers. Besides these, the optimal operation of other DH components was also studied in [29]. Lamaison et al used mixed integer linear programming and the multi-objective parametric optimization method to study a district heating system that consists of a biomass generator, a heat-pump and heat storage in the French energetic context [30]. The electrification of heating systems can be a great obstacle for DH. In paper [31], authors analysed if ground source heat pumps could replace the existing DH systems in Sweden. They concluded that a complete replacement of DH with geothermal heat pumps is unrealistic. Paper [32] uses three types of systems to simulate how increasing the share of heat pump production influences DH systems when optimized for the lowest production costs. The findings of the simulations together with insights from the interviews imply that the viable amount of heat pump-based heat production in DH systems would be around 10-25% in Finland, which is much higher than the current 3%.

While many researchers explore the optimal supply capacities of power-to-heat technologies, they rarely analyse the impact of various parameters on power-to-heat supply capacities, such

as electricity market prices or power sector emission factors. These two parameters are greatly influenced by the penetration of variable renewable energy sources. Paper [33] shows the relationship between variable RES production and electricity market prices by using the EnergyPLAN tool for the modelling and simulation of energy systems. Amiri et al used a linear programming model to analyse a district heating system connected to the European power market [34]. They showed that interconnection with other heating systems can reduce the overall system cost. In [35], the electricity market in renewable energy systems was discussed and modelled. The case study was based on an energy system of Denmark with a 100% RES system for year 2050. Felten developed the model framework for the analysis of a coupled heat and power sector in large scale systems, such as the EU [36]. The model can provide a cost optimal dispatch and unit commitment of various technologies. In paper [37] the drivers of electricity prices spot markets were analysed and modelled on the example of the German power sector. Liu et al analysed marginal cost pricing for competitive district heating. In the paper, DH participates in the power market with cogeneration (CHP) and heat pump units. Dispatch, i.e. unit commitment was modelled by using the PLEXOS tool. It should be mentioned that power market prices are taken as the input data, i.e. it was assumed that the participating CHP and heat pump units do not shift the market equilibrium [38]. Hennessy et al [39] analysed the techno-economic feasibility of commercial power-to-heat technologies in DH systems by taking into account different various forecasts of spot market prices. However, the spot market prices were not modelled and only system operation was taken into account, while utilizing predefined capacities and technologies. In paper [40], authors analysed an integrated demand response while analysing the heat and electricity market price by optimizing bidding strategies, i.e. maximizing the net revenue of the supplier. Yifan et al modelled DH system connection with the power sector by analysing the operational flexibility of each local DH system through CHP and power-to-heat units. They showed how operational flexibility from multiple DH systems can effectively improve wind power integration [41]. Zhang et al proposed a two-layer optimization model to find out the optimal configurations of clean-heating improvements in a district energy system with high penetration of wind power. Their research focused on the implementation of power-to-heat technologies in combination with thermal storage units [42]. Fabian Levihn presented an empirical analysis of power and heat market integration from the DH network in Stockholm. The mentioned system utilizes CHP and power-to-heat units while at the same time participating in the stabilization of the power network by offering negative and positive power ramping [43]. Ma et al provided reviewed sources of flexibility in district heating systems. Power-to-heat technologies connected to the power market are a great source of flexibility [44]. Yifan et al developed a model capable of exploring electric flexibility coming from the district heating system, thus enabling increased wind penetration [41]. The model was validated on an integrated power and heating system consisting on numerous CHP and thermal power units and wind farms. In paper [45], a two-stage modelling approach was used to investigate the real-time flexibility of cogeneration power plants in district heating systems. In the first stage, the heat production plan of a CHP plant was derived to minimize the system heat cost in a deregulated heat market by using its flexibility; in the second stage, the CHP plant was dispatched to provide a real-time balancing service with the remaining flexibility.

Åberg et al. [46] provided a detailed analysis on how market prices influence the operation of power-to-heat technologies in the case of Sweden. They used historical price curves and added wind and solar capacities in order to analyse the shift of the supply curve, thus achieving new

electricity market prices. For the newly achieved prices they ran an analysis of power-to-heat operation units and drawn the following conclusions: the results show that power-to-heat production is significantly increased (up to 98%) when electricity prices are influenced by variable RES production. Besides spot prices, the power market also enables participation in an ancillary services market. This is excellent opportunity for power-to-heat technologies. Terreros et al provided an analysis of different electricity market options for heat pumps in rural DH networks in Austria. The optimal bidding strategy for heat pumps is buying 50% of the energy in the spot day-ahead market and offering 50% of the capacity for the negative balancing automatic frequency restoration reserve [47]. Thermal storage further increases the production of power-to-heat technologies by up to 46%. Paper [48] analysed the introduction of heat pumps with heat storage in a small district heating system while considering integration with a power market. They concluded that a thermal storage size can reduce the annual costs of a system effectively but can easily be oversized. In paper [49], authors demonstrated that electric boilers, which are part of a DH system, are capable of providing negative secondary control power in a flexible and a cost-effective manner. An analysis for the German energy system was carried out. Ito et al [50] analysed the role of DH cogeneration units for the purpose of maintaining grid stability. Particle swarm optimization was used in order to acquire the optimal operation of the DH system. In paper [51], a novel method for a heat and power dispatch model was proposed which also involved the thermal inertia of the system. The acquired results have shown how wind energy integration could be increased by utilizing the thermal inertia of a DH system. Gravelsins et al [52] used a system dynamics approach in order to investigate how solar photovoltaics could be integrated into DH systems to achieve economically feasible and flexible energy production by using power-to-heat technologies. Leitner et al [53] provided a method that enables a detailed technical assessment of the operation of coupled heat and power networks. Moser et al designed a heat market that is based on a merit order to evaluate industrial waste heat in DH systems. They showed that power market prices can drastically change merit order, especially during summer when heat loads are reduced [44]. Dominković et al developed dynamic pricing models for DH systems in Denmark and Finland [54]. It was shown that electricity prices have a high impact on carbon dioxide (CO_2) emissions and average marginal prices for both systems. Study [55] analyses how different electricity grid tariff structures will affect the flexible use of electricity in future Nordic district heating systems. Paper [56] summarises operation experiences of Swedish heat pumps to support and facilitate the planning of future power-to-heat solutions with heat pumps in DH systems. The authors showed that older heat pumps operate with lower utilisation capacity due to competing technologies such as cogeneration units in DH systems. In paper [57] authors used energyPRO to analyse three low-temperature DH schemes, where a booster heat pump was utilized with various thermal sources. An analysis of spot market prices reduction was not taken into account. Paper [58] uses EnergyPLAN to analyse how a shift from individual electric heating to DH affects the flexibility that the Norwegian energy system can provide to Europe. Paper [59] analyses how a Swedish municipality can contribute to lowering peak electricity demand by utilizing DH. It was shown that the choice of heating system is more important than reducing the heat demand itself to lower electricity peak demand in the future. Sorknæs et al [60] introduced the concept of a smart energy market. The authors illustrated and quantified how future renewable heating, green gas and liquid fuel markets will influence the electricity markets and vice versa. Mirzaei et al evaluated integrated power, heating and gas networks by developing a multi-network unit commitment model in

combination with storage technologies [61]. The goal is to minimize the operation costs of an integrated electricity, gas and DH system while satisfying the constraints of all three networks. In paper [62], the European heat demand was combined with a Dispa-SET power system model to evaluate a coupling pathway in terms of operating costs, efficiencies and associated CO_2 emissions. The results showed that the conversion of thermal into CHP plants increases efficiency and reduces both the operating costs and the environmental impact of the energy system.

1.4. Scientific contribution

Numerous papers dealing with multi-objective optimization of DH often do not optimise the system capacity regarding the power market prices change. In the majority of papers dealing with power and DH sector integration, spot market prices are rarely modelled, but considered through different scenario analyses. Due to this, most papers cannot provide the results on the impact of wind penetration on DH parameters. Nevertheless, paper [46] succeeded in displaying the impact of wind integration on district heating operation and demand response potential. However, the mentioned paper did not consider power-to-heat and thermal storage capacity optimization, but focused only on system operation acquired by using single-objective optimization.

The main scientific contribution of this paper is the analysis of an impact of a wind production increase in a power market on optimal power-to-heat and thermal storage capacities in a local DH system by using a multi-objective optimization approach. Furthermore, the power market clearing prices have been modelled by using publicly available historical bidding curves data in order to analyse the impact of wind production penetration. Finally, this paper provides a potential answer to the following questions:

How does wind penetration in a power market:

- shift the solution of the district heating multi-objective optimization, i.e. its Pareto front?
- impact optimal power-to-heat capacities in a district heating system for different Pareto optimal solutions?
- influence the optimal thermal storage size in a district heating system for different Pareto optimal solutions?
- affect the operation of the district heating system for different Pareto optimal solutions?

The paper is divided in following way. In Section 2, the method is explained. Section 3 shows the input data related to district heating optimization and the calculation of power market prices. Furthermore, Section 3 provides an overview of the proposed scenarios. Section 4 displays the main results obtained in this paper. Section 5 concludes the paper and displays the most important results obtained within this research.

2. Method

The overview of the method used in this paper is shown in Figure 1. The overall approach can be divided into two interconnected models: the district heating model and the modelling of the market clearing price under the influence of wind energy penetration. Market clearing price modelling is carried out by using known power market bidding curves and wind production data. In order to run the district heating model, several inputs are needed: district heating load, technology characteristics, such as efficiency and ramping limits, and prices (investment, fuel and operational costs). Besides these, every technology has a CO_2 emission factor that is related to the fuel. In the case of power-to-heat technologies, electricity is used as a fuel.

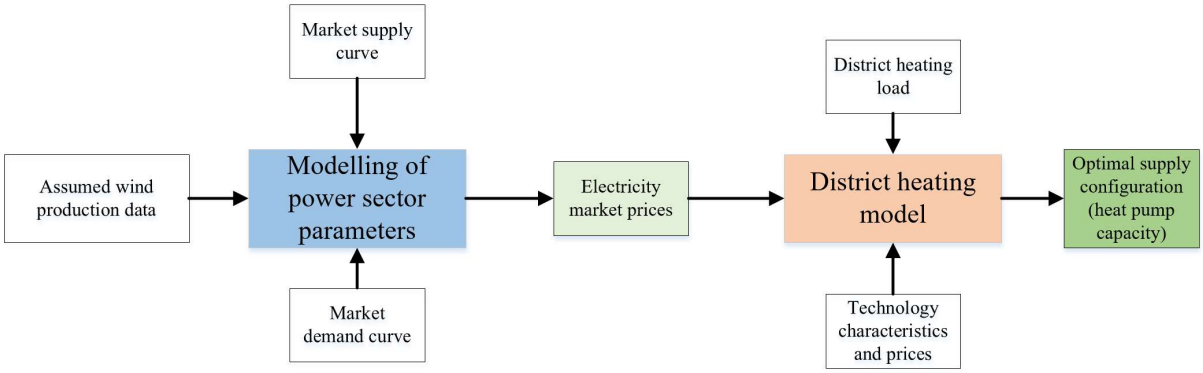

Figure 1 Overview of the method

2.1. District heating model

The district heating model used in this research is based on the model developed in the authors' previously published papers [63], [64]. The model is used for a multi-objective optimization of district heating systems with respect to the total costs and CO_2 emissions. It can be used to optimize supply capacities, including thermal storage size, and the hourly operation of the system for a whole year. The model can choose between various supply units, such as heat-only boilers, cogeneration, electrical heaters, heat pumps and solar thermal collectors. Two fuels can be used: natural gas or biomass. The optimization variables of the model are supply capacities P_i, thermal storage size TES_{size} and the hourly operation of each supply source $Q_{i,t}$ and thermal storage charging and discharging $TES_{in-out,t}$ where i represents the technology type and t the time step. The latter is equal to one hour, while the time horizon is equal to 8,760 hours, i.e. whole year. The model also includes various constraints, which are presented below.

Equation (1) presents the most important constraint which states that the hourly demand DEM_t should be covered with various supply technologies $Q_{i,t}$ where i represents the technology type. The operation of the thermal storage is defined with charging or discharging, i.e. $TES_{in-o\ ,t}$. If the storage discharges, the term $TES_{in-out,t}$ is negative and if thermal storage is charging, the term $TES_{in-ou\ ,t}$ is positive. This is why in Equation (1), thermal storage terms have negative signs. Finally, it should be mentioned that this model includes two thermal storages. The first one is used as the buffer (short-term thermal storage) and the other one could act as the seasonal storage which could be charged solely by solar thermal technology. The connection between all the technologies is shown in Appendix.

$$DEM_t = Q_{HOB,gas,t} + Q_{HOB,biomass,t} + Q_{EH,t} + Q_{HP,t} + Q_{CHP,gas,t} + Q_{CHP,biomass,t} - TES_{1,in-out,t} - TES_{2,in-out,t} \quad (1)$$

Equation (2) presents the constraint that links the supply capacity P_i and the hourly operation of technology $Q_{i,t}$. The technology output on an hourly level cannot be higher than technology installed capacity.

$$0 \leq Q_{i,t} \leq P_i \quad (2)$$

In order to provide a more realistic operation of the system, ramping limits are put on each technology, as shown in Equation (2), where $r_{up-down,i}$ presents the ramping limit of technology i. It is defined as the percentage of the supply capacity that could be ramped up or down in a single hour.

$$-r_{up-down,i} \cdot P_i \leq Q_{i,t} - Q_{i,t-1} \leq r_{up-down,i} \cdot P_i \quad (3)$$

The thermal storage operation is defined with Equations (4) and (5). Equation (4) presents the constraint put on the state of charge (SOC_t) of a thermal storage in the first and the last hour of the optimization time horizon, i.e. they should be equal. Furthermore, the model allows defining the percentage of the state-of-charge by using the $SOC_{start-end}$ parameter. For the purpose of this paper, it is defined to 50% of the thermal storage size (TES_{size}). Equation (5) shows the hourly operation of the thermal storage. The state-of-charge in a time step t is equal to the state-of-charge in the previous time step $(t-1)$ increased by the thermal storage charge (positive term) or discharge (negative term) and reduced by the thermal storage loss in the respective hour. The losses are defined with the loss factor TES_{loss}. Finally, the thermal storage state-of-charge SOC_t cannot be higher than the thermal storage size TES_{size}, shown in Equation (6). In other words, the optimal thermal storage capacity is equal to the highest SOC_t value.

$$SOC_{t=1} = SOC_{t=8760} = SOC_{start-end} \cdot TES_{size} \quad (4)$$

$$SOC_t = SOC_{t-1} + TES_{in-out,t} - SOC_t \cdot TES_{loss} \quad (5)$$

$$SOC_t \leq TES_{size} \quad (6)$$

While all technology capacities are defined with peak thermal power, the solar thermal capacity is defined with the total solar thermal area A_{ST}. Equation (7) shows the connection between the hourly operation of the solar thermal and its total area. It should be noted that the solar thermal operation is tightly constrained and depends on the optimized total solar area A_{ST} and the predefined hourly specific solar thermal output $P_{solar,specific,t}$.

$$Q_{ST,t} = A_{ST} \cdot P_{solar,specific,t} \quad (7)$$

The specific solar thermal output can be calculated by using Equation (8), where $\eta_{c,t}$ represents the solar thermal collector efficiency in a time step t, while G_t is global solar irradiation in a time step t. The last term also represents the hourly input data of the model which can be acquired by using publicly available data such as PV GIS [65] developed by JRC or other available databases [66].

$$P_{solar,specific,t} = \eta_{c,t} \cdot G_t \quad (8)$$

The calculation of solar thermal collector is obtained by using Equation (9) based on the European standard EN12975 [67], where η_0 represents optical efficiency (without thermal losses), a_1 is the first order heat loss coefficient and a_2 is the second order heat loss coefficient, while T_m represents the mean collector fluid temperature. The mentioned parameters depend on the collector type and can be obtained by checking the manufactures' factsheets which can be found in publicly available databases [68]. Finally, $T_{ref,t}$ is the outside air temperature for the given location which can be obtained by using the already mentioned publicly available databases [65], [66].

$$\eta_{c,t} = \eta_0 - a_1 \frac{\left(T_m - T_{ref,t}\right)}{G_t} - a_2 \frac{\left(T_m - T_{ref,t}\right)^2}{G_t} \tag{9}$$

The efficiency of the heat pump can be calculated by using Equation (10) [25]. It is based on the temperature difference between the heat source (air, $T_{ref,t}$) and the heat sink (DH supply network, $T_{DH,t}$) temperature multiplied with the Lorentz factor $f_{Lorentz}$. The district heating supply network temperature is not constant, but depends on the outside air temperature as shown in [69].

$$\eta_{HP,t} = f_{Lorentz} \cdot \left(\frac{T_{DH,t}}{T_{DH,t} - T_{ref,t}}\right) \tag{10}$$

It should be noted that solar thermal collector and heat pump technologies do not have constant efficiency as other supply sources, since they can be calculated prior to the optimization procedure. All other technology efficiencies are treated as constants in order to secure the linearity of the model. The problem is written as a linear programming (LP) model by using the Julia programming language and the linear programming solver called Clp.

An overview of the district heating model is presented in Appendix.

2.2. Objective functions

As already mentioned, this paper deals with multi-objective optimization. The goal of the optimization model is to minimize the economical, f_{econ}, and ecological, f_{ecol}, objective function, as shown in Equation (11).

$$\min(f_{econ}, f_{ecol}) \tag{11}$$

The economical objective function represents the total costs of the system that can be calculated by using Equation (12). $C_{investment,i}$ is the discounted investment costs of technology i. It should be noted that it does not have a temporal summation since it is paid only once. $C_{fuel,i,t}$ represents fuel costs, while $C_{O\&M,i,t}$ is operation and maintenance costs for technology i in a time step t. The last term on the right in the brackets $Income_{i,t}$ represents additional income due to the electricity sold on the market by using cogeneration units.

$$f_{econ} = \sum_i C_{investment,i} + \sum_{t=1}^{t=8760} \sum_i \left(C_{fuel,i,t} + C_{O\&M,i,t} - Income_{i,t}\right) \tag{12}$$

The ecological objective function is defined as the total CO_2 emissions of the district heating, which is obtained by using Equation (13). The specific emission factor, $e_{CO_2,i}$ is defined per fuel, while η_i is technology efficiency.

$$f_{ecol} = \sum_{t=1}^{t=8760} \sum_{i} (e_{CO_2,i} \cdot Q_{i,t} / \eta_i) \quad (13)$$

2.3. Multi-objective optimization

Before explaining the method used for handling multi-objective optimization, the crucial issue related to such optimization should be mentioned. It is impossible to simultaneously acquire the minimum of both objective functions. By acquiring the minimum of the first, the highest value of the second one will be reached and vice-versa. Thus, the solution of multi-objective optimization is not a single value but a whole set of them, which lie on the same front, the so called Pareto front. It could be understood as the compromise between two objective functions – approaching to the minimum of one is only possible at the expense of other objective function.

In order to deal with multi-objective optimization, and to construct the Pareto front, the epsilon constraint method has been used in this paper [70]. It is based on translating the multi-objective optimization problem into single-objective optimization by introducing an additional set of constraints put on the second objective function, as shown in Equation (14). Parameter ε_{ecol} represents (epsilon) constraint put on the ecological objective function, while the economical objective function is minimized. By changing ε_{ecol}, different solutions are achieved that lie on the Pareto front [70]. Due to this, the resolution of the Pareto front depends on the number of optimization runs. It is important to mention that ε_{ecol} should be in the feasible region. To define the feasible region, boundaries of the Pareto front should first be acquired.

$$\min (f_{econ}) \text{ for } f_{ecol} \leq \varepsilon_{ecol} \quad (14)$$

2.4. Market price modelling

In this paper, power-to-heat optimal capacities are analysed with regard to electricity market prices. These prices also represent an input for the district heating model. The market price was modelled with respect to wind energy penetration by using publicly available market bidding data, i.e. supply and demand market curves for each hour of the year, as explained below. The mentioned approach has also been implemented in this paper to avoid challenging power market modelling which involves detailed unit commitment and dispatch on a power plant level for a whole market on an hourly level for a whole year.

Market clearing price modelling by using supply and demand market curves has been previously shown in [46] and [71]. In paper [71], the focus was put on analysing the increase of demand on the market clearing price, i.e. the buy curve was shifted in order to obtain the new (modelled) market clearing price. In paper [46] the authors used a similar approach, but this time, the supply curve has been shifted in order to model the influence of the increased variable RES production. For the purpose of this paper, the method shown in [46] was used. However, only the wind production increase is studied since these capacities are the most promising in the analysed Nord Pool market. Finally, it is assumed that the marginal price of wind is equal to zero.

To fully understand the approach used, the market model should be explained. For this purpose, Figure 2 will be used. It represents the market situation for a single hour and must be constructed 8,760 times per year. The power or electricity market operates as any other market of goods. Two major parameters first have to be understood: the trading volume (x-axis, in MWh) and the market price (y-axis, in EUR/MWh). For every volume, the market price can be defined, which is called a "bid". The set of all bids creates the bidding curve. In Figure 2, two curves can be noted. The blue full curve represent the supply curve ("sell curve"). In the power market, the supply is represented with power plant operators: condensation power plants, cogeneration units, wind turbines, photovoltaics, etc. Since renewable energy sources have low operational costs, they can offer the trading volume at a lower price, even reaching zero or negative values. The red curve represents the demand curve ("buy curve"). Where these two curves intersect, the market clearing price and the respective trading volume are obtained. In Figure 2, this is marked with yellow dot. As already mentioned, variable renewable energy sources, e.g. wind, have low operational costs, thus offering bids at a lower price. If additional wind is introduced into the market, the supply curve is shifted to the right. In Figure 2, this is represented with the dotted blue line. Due to the shift of the supply curve to the right, the new market clearing price is obtained (marked with a green star), which is lower than the reference one. This represents the crucial effect of variable renewable energy sources integration, since it opens additional opportunities for demand response, power-to-heat, power-to-X, and other technologies that could participate on the market.

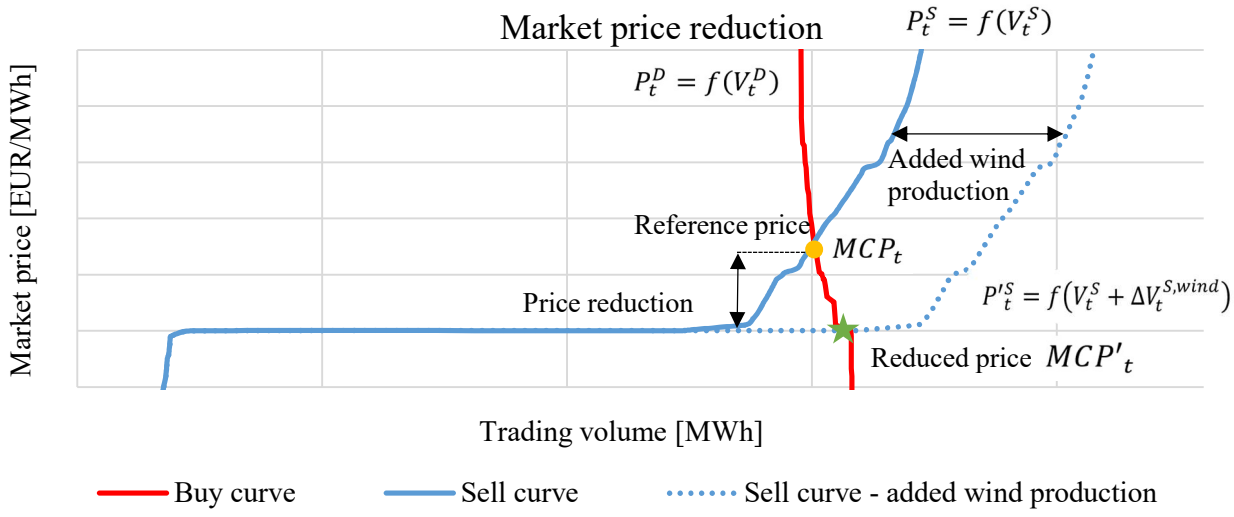

Figure 2 Illustration of the market price reduction method for a single hour

The market price modelling can also be represented with the following equations. Let us assume that price P_t in a time step t is a function of a volume participating on the market. Equation (15) shows the generic correlation between the (supply) price P_t^S and the supply volume V_t^S, while Equation (16) shows the connection between the buy (demand) price P_t^D and the demand volume (V_t^D). The market clearing price MCP_t is achieved for the market equilibrium, as shown in Equation (17). In this paper, the penetration of wind energy production into the power market is analysed, which is marked with $\Delta V_t^{S,wind}$ in Equation (18). Due to this, an updated price curve P'^S_t is acquired, as shown in Equation 17. Since the updated price curve is shifted, the new market clearing price MCP'_t is obtained as shown in Equation

(19). Since the added wind production has zero marginal costs, the new market clearing price is lower than the reference one, as shown in Equation (20).

$$P_t^S = f(V_t^S) \tag{15}$$
$$P_t^D = f(V_t^D) \tag{16}$$
$$MCP_t = P_t^S = P_t^D \tag{17}$$
$$P'^S_t = f\left(V_t^S + \Delta V_t^{S,wind}\right) \tag{18}$$
$$MCP'_t = P'^S_t = P_t^D \tag{19}$$
$$MCP'_t < MCP_t \tag{20}$$

Although this approach has been used in previously published papers [46], [71], it has some major drawbacks related to market evolution and power system dynamics:

- Buy (demand) curves are not updated, i.e. they stay the same for all levels of wind penetration.
- The acquired market clearing price represents the system price. According to [72], the system price is an unconstrained market clearing reference price. It is calculated without any congestion restrictions by setting the transfer capacities to infinity. In reality, different zones will not achieve price convergence due to the limited transfer capacities.
- Due to the lack of unit commitment and dispatch modelling, negative prices could not be obtained by using this approach.
- The impact of ramping, starting and shut-down costs cannot be obtained by using this approach since the system dynamics are not taken into account.
- The assumed running costs of wind production are equal to zero. However, there are small operation and maintenance costs.
- Since this approach does not include hourly power dispatching and unit commitment, the impact on reversible hydro storage capacities could not be taken into account.

From the drawbacks presented above, it can be concluded that the market clearing prices obtained by using this approach represent an idealized case. The major issue is the lack of dispatch and unit commitment modelling and neglecting the so-called cycling costs. These expenditures are related to starting, ramping and forced outage costs. It should be mentioned that the cycling costs mainly depend on the technology, as shown in [73]. The direct start costs can be in range from 5 EUR/MW for combined cycle natural gas turbines, up to 35 EUR/MW for nuclear power plants. Similarly, the ramping costs are equal to 0.5 EUR/MW for natural gas power supply units and 1.8 EUR/MW for coal power plants. In other words, the impact of wind and solar penetration on the cycling costs, greatly depends on the power supply technology mix. Paper [73] analysed the cycling cost for the German power system under the largescale integration of intermittent renewable energy sources, i.e. wind and solar. The cycling costs almost doubled (from 5 to 10 million EUR/week) for the wind and solar energy penetration increase from 0% to 50%. The largest contribution in the cost increase comes from the starting costs. Nevertheless, it should be noted that the total costs are reduced from 170 to 80 million EUR/week for the wind and solar share equal to 50%. The share of the cycling costs in the total generation costs is kept relatively low but increases steadily from 3% up to 15% for

a large penetration (50% share) of wind and solar. However, in this paper, the maximum wind share is much lower, equal to 21%.

Since the approach used in this paper does not include the cycling costs, it can be expected that obtained average market prices in this paper are slightly underestimated.

3. Case study

This section presents the input data needed for market price modelling. Furthermore, it includes DH system parameters needed for carrying out optimization, such as hourly distributions and technology related parameters, prices, etc. Finally, the two scenarios developed for the purpose of the analysis are also presented.

3.1. Input data

The model developed for the purpose of this paper was tested on a numerical case study of a DH system. The input data used in the analysis can be divided in hourly distributions and single-value parameters. Several hourly distributions are needed, such as: heating and domestic hot water demand, outside air temperature, global solar irradiation, specific wind power production and finally, electricity market prices, which are calculated by using the method described in Section 2.

Other district heating parameters, such as specific investment, fuel and O&M costs, the fuel emission factor, technology efficiencies, ramping limits, power-to-heat ratio for cogeneration and technical life time can be seen in Table 1 [74]. In Appendix, the hourly DH demand is shown.

Table 1 Technology data

Technology	Investment costs [€/MW] / [€/m^2] /[€/MWh]	Fuel cost [€/MWh]	Variable costs [€/MWh]	Emission factor [tonnes of CO_2/MWh]	Efficiency/ storage loss [-]	Ramp-up/down [-]	Technical lifetime [years]	Power-to-heat ratio [-]
Natural gas boiler	100,000	20	3	0.22	0.9	0.7	35	-
Biomass boiler	800,000	15	5.4	0.04	0.8	0.3	25	-
Electrical heater	107,500	Electricity market	0.5	0.293	0.98	0.95	20	-
Heat pump	680,000	Electricity market	0.5	0.293	Hourly distribution	0.95	20	-
Cogeneration natural gas	1,700,000	20	3.9	0.22	0.5 (thermal)	0.3	25	0.82
Cogeneration biomass	3,000,000	15	5	0.04	0.6 (thermal)	0.3	20	0.55
Solar thermal	300 €/m^2	0	0.5	0	Hourly distribution	-	25	-
Thermal storage, buffer	3,000 €/MWh	0	0	0	1% (loss)	-	25	-
Seasonal thermal storage	500 €/MWh	0	0	0	0.1% (loss)	-	25	-

To obtain the market clearing price, the demand and supply curves are needed for every hour of the year. They can be acquired by using publicly available Nord Pool bidding data [72]. For every hour of the year, the Nord Pool database publishes set of purchase and sell bids which enables the development of the bidding curves similar to the one shown in Figure 3. In order to acquire the market clearing price for the given hour, an intersection of the mentioned curves

has to be found. This procedure is repeated for every hour of the year, thus providing the district heating model with 8,760 values. Of course, for the reference year, the hourly market price is already available.

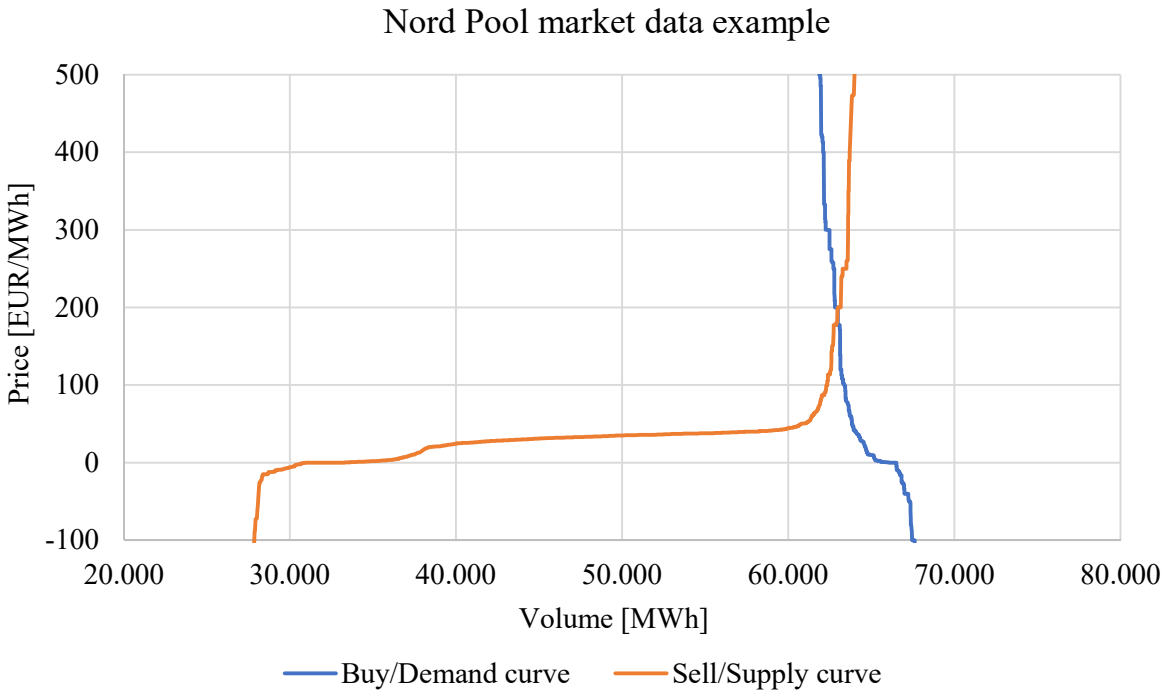

Figure 3 Nord Pool data example for a single hour [72]

One of the objectives of this paper is to analyse how increased energy production affects electricity market prices. As already explained in Section 2, the method is based on adding zero-cost volumes in the supply bid curve to obtain the new market clearing price. However, for the analysis of additional wind energy production, the hourly data for wind is also needed. In this paper, the already existing Nord Pool historical wind production data for the reference year has been used in order to acquire the predefined total yearly wind energy production [72]. Figure 4 shows the relative wind production used in this paper in order to scale the reference one and obtain the predefined total yearly wind production shown in Table 2. The relative wind power was obtained by dividing the hourly wind production, obtained for the reference year 2018 from the Nord Pool database, by the respected maximum wind production in the given year. In that case the value of 1 represents the maximum hourly wind production in that year, while the value zero represents no wind production. This hourly relative wind power distribution was used to obtain the hourly wind production for different levels of wind penetration as shown in Table 2, i.e. for 45, 60, 75 and 90 TWh of wind production. These values were then used to shift the historical Nord Pool supply curves and obtain the new (reduced) market clearing prices.

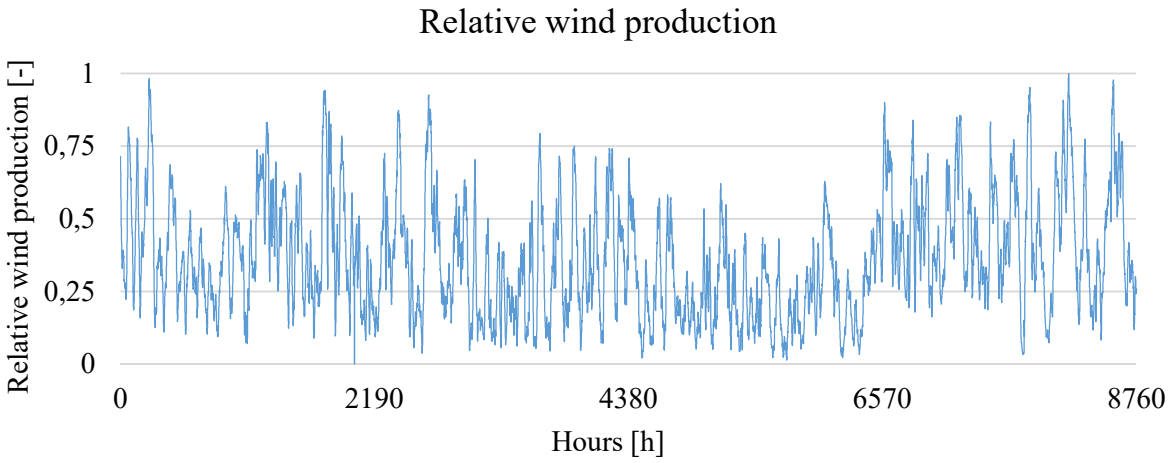

Figure 4 Relative wind production

3.2. Scenario analysis

For the purpose of this paper, two scenarios have been developed, as shown in Table 2. In Scenario 1 the power sector emission factor is taken as the historical value for Denmark, since it is assumed that it is the location of the numerical example of a new local district heating system. In the second scenario it is assumed that the power sector emission factor is equal to zero, i.e. power-to-heat units do not have CO_2 emissions. This presents an ideal case where the power sector utilizes only renewable energy sources. Furthermore, by obtaining the results with this assumption, the ideal system, which is not bounded with power sector emissions, can be analysed. For both scenarios, five levels of wind penetration have been studied. The reference case presents the historical data for the year 2018, where wind energy production was equal to 33 TWh. The electricity market prices have been recalculated for different levels of wind production penetration: 45, 60, 76, and finally, 90 TWh. The wind share is equal to 8% for the reference case and 11%, 14%, 18% and 21% for other wind penetrations, respectively. It is calculated with respect to total production for the year 2018.

Table 2 Scenario description

Scenario name	**Power sector emission factor [tonnes of CO_2/MWh]**	**Wind energy penetration**
Scenario 1	0.29	Electricity market prices are recalculated by considering penetration of wind energy production: - 33 TWh of wind penetration – Reference case (wind share of 8%) - 45 TWh of wind penetration (wind share of 11%) - 60 TWh of wind penetration (wind share of 14%) - 75 TWh of wind penetration (wind share of 18%) - 90 TWh of wind penetration (wind share of 21%)
Scenario 2	0	

4. Results and discussion

Section 4 is divided into several parts. In Section 4.1, the market price reduction results are explained and analysed in more detail. In Section 4.2 and Section 4.3, the optimal heat pump capacities and the Pareto front shift for different levels of wind penetration are discussed for both scenarios. Finally, Section 4.4 provides a comparison of district heating supply system operation for different levels of wind penetration and district heating system CO_2 emissions.

4.1. Market price reduction

As shown in Section 2, the integration of intermittent renewable energy sources reduces power market prices, due to their zero-marginal prices. This has also occurred in this study with the penetration of additional wind capacities in the Nord Pool market. The reference wind penetration was equal to 33 TWh, which presents an 8% share of the power production. Wind energy production was increased up to 90 TWh with the step equal to 15 TWh. Figure 5 shows the duration curves of hourly market prices for different levels of wind penetration. First of all, it can be noted that the peak market price drastically falls from 199 EUR/MWh for 33 TWh of wind production down to around 60 EUR/MWh for higher wind penetration levels. Furthermore, it is evident that the number of nearly-zero-price hours increases with wind penetration, as explained below.

The peak market price for the reference wind penetration of 33 TWh is relatively high, equal to 199 EUR/MWh. Such high market clearing prices are probably caused by a non-predicted external event. The bidding curves for this specific hour are shown in Figure 3. It can be seen that the demand curve intersects costly (peaking) supply technologies, resulting in a high market clearing price. It can be also noted how a small shift of the supply curve to the right (by adding a low-cost technology such as wind) drastically reduces the market clearing price. This actually happened in this paper. Unfortunately, the nature of unpredicted events is not considered in this analysis. However, those events are already integrated in the historical bidding curves and are taken into account as such.

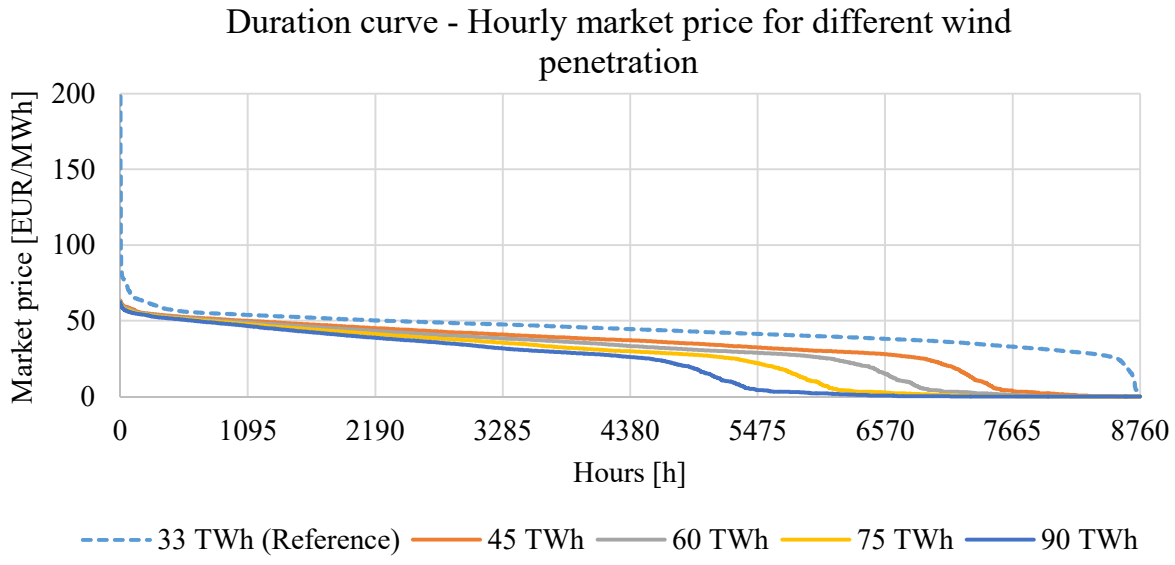

Figure 5 Duration curve of hourly market price for different values of wind penetration

Figure 6 shows the average market price and the number of zero-price-hours for different levels of wind penetration. The average market price for reference wind penetration is equal to 44 EUR/MWh. It decreases down to 22 EUR/MWh for wind penetration level of 90 TWh. It can be noted that the average market price does not fall linearly with a wind penetration increase but potentially reaches saturation. On the other hand, number of zero-price hours follows the trend of quadratic increase. The reference wind penetration has no zero-price hours, while for wind penetration of 90 TWh the number of zero-price hours reaches around 1,500. The possible reason behind this great number of zero-price hours is the following. In real markets, supply bids are not exactly 0 EUR/MWh. They are usually around this value, probably due to different operation and maintenance costs of the renewable energy source technology.

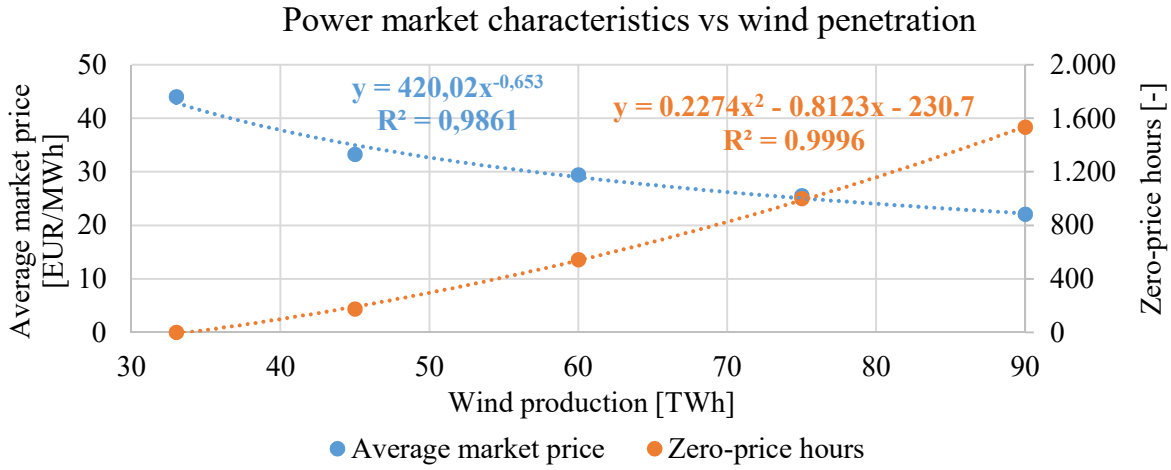

Figure 6 Average market price and zero-price hours for different wind penetration values

A more detailed comparison of power market prices is shown in Figure 7 and Figure 8. They show the hourly market price distributions for a winter and a summer week, respectively. First of all, it should be noted that the summer week obtains more zero-price hours than the winter period. The peak market prices do not differ greatly for different levels of penetration, but on the other hand the market price drops significantly in the periods of lower reference prices, i.e. when there is wind production.

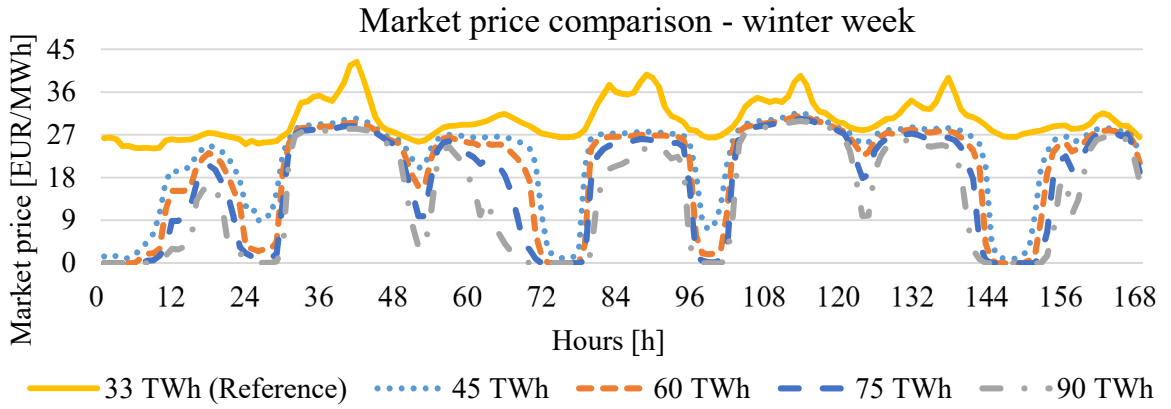

Figure 7 Market prices comparison for different wind penetration values – winter week

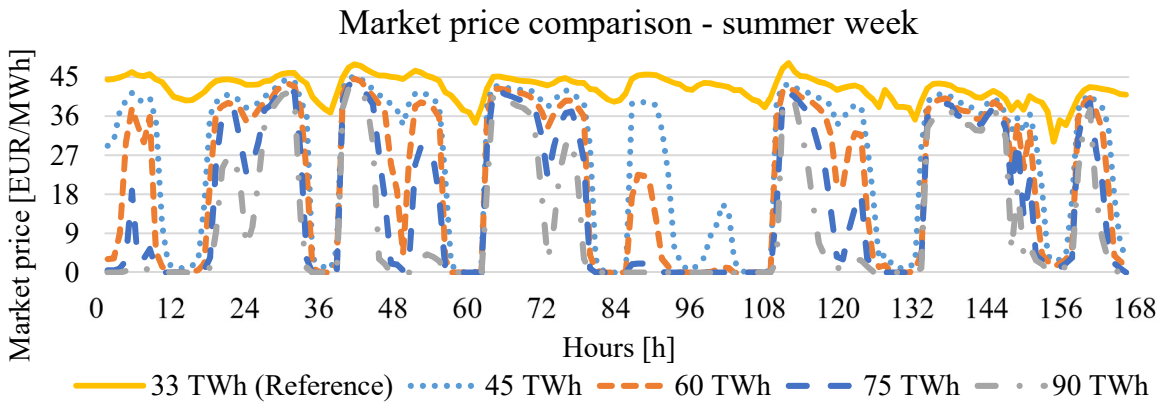

Figure 8 Market prices comparison for different wind penetration values – summer week

4.2. Optimal heat pump parameters – Scenario 1

As already mentioned in Section 2, the result of multi-objective optimization is not a single value but a whole set of them which lie on the so-called Pareto front. Figure 9 shows the Pareto front for Scenario 1, where the assumed power sector emission factor is equal to 0.29 tonnes/MWh. It is important to mention that the most environmentally friendly solution is not shown in this figure since it is off-scale, i.e. it reaches high total costs and is not of interest in this analysis. As explained in Section2, the Pareto front is constructed by using the epsilon constraint method, i.e. by obtaining a definite number of points which lie on the Pareto front. It can be seen that the epsilon constraints are equal to 6,000, 5,000 and 3,000 tonnes of CO_2 emissions. On the other hand, the most-left solutions present the most economically feasible solutions, which also emit the highest amount of CO_2. It can be noted that the penetration of wind production shifts the Pareto front to the region of lower emissions and lowers the total costs due to the increased utilization of heat pumps as can be seen in Figure 10.

Pareto fronts can also represent the savings in total costs and CO_2 emissions. The reference case includes reference power market prices with reference wind penetration. However, with additional wind production, lower market clearing prices are obtained and heat pumps become a more economically viable solution. Savings in this case refer to CO_2 emissions and system cost reductions. These savings in Scenario 1 are the most visible in Pareto front shifts in Figure 9. For the same levels of CO_2 emissions, the system cost reduction is obtained. In Scenario 1, the maximum cost reduction is around 70,000 EUR for a CO_2 emission level equal to 6,000 tonnes.

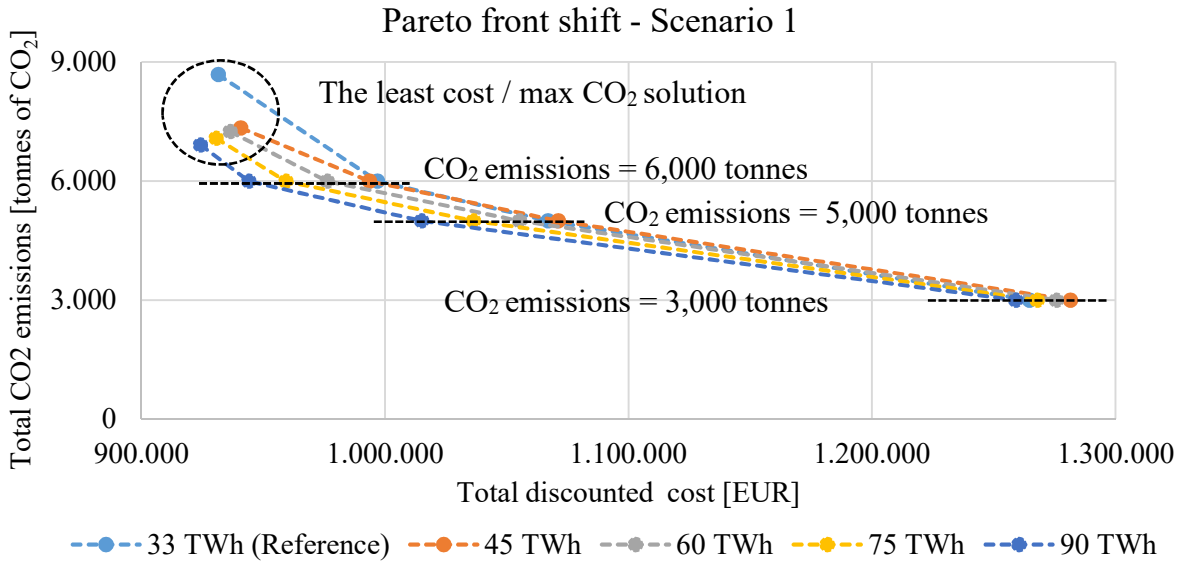

Figure 9 Pareto front shift for different wind penetration values – Scenario 1

Figure 10 shows optimal heat pump capacities for different levels of wind penetration and CO_2 emissions values. The trend is obvious: the increase of wind penetration allows larger heat pump capacities from the economical point of view. It should be noted that for reference wind penetration of 33 TWh, a heat pump is not part of the optimal solution for any CO_2 emission value. The highest heat pump capacity increase is evident for CO_2 emissions equal to 5,000 and 6,000 tonnes. For these values, the optimal heat capacity reaches around 4 MW for wind

penetration of 90 TWh. For lower CO_2 emissions, the optimal heat pump capacity is reduced due to the power sector emission factor, and more environmentally friendly technologies are used, such as solar thermal collectors or biomass boilers.

A similar trend can also be observed in Figure 11, which shows the optimal heat pump production, i.e. the thermal energy produced by using a heat pump. It can be noted that the resulting load factor is always around 0.6 as seen in Figure 12. It is to be expected that lower market prices will allow more frequent operation of power-to-heat units, especially during the night and during periods of low or even zero-price hours. In order to successfully achieve this, thermal storage is needed. In this paper, we have analysed the impact of a wind penetration increase on the optimal thermal storage size of a local district heating system. This trend is shown in Figure 13. As expected, lower power market prices cause an increase in thermal storage size used for heat pump utilization, especially during night periods, as shown in Section 4.4 in more detail.

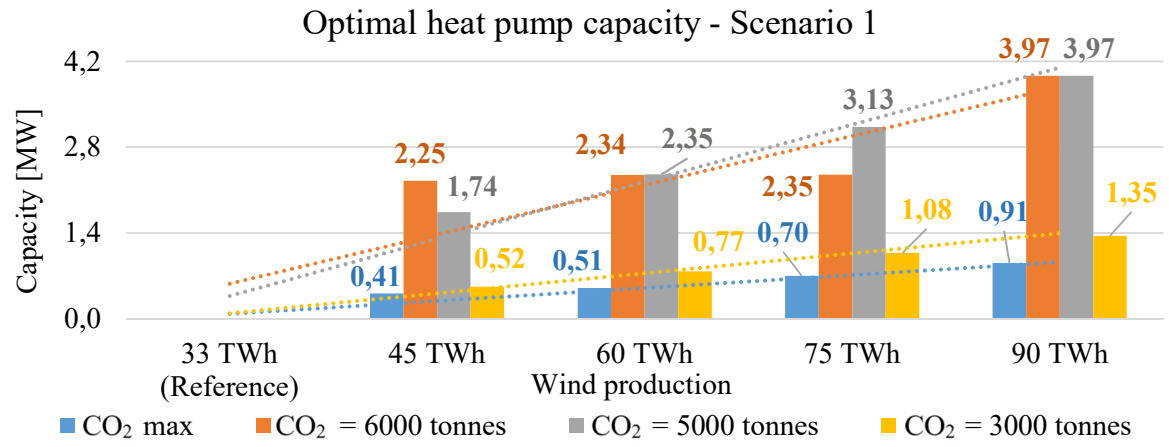

Figure 10 Optimal heat pump capacities – Scenario 1

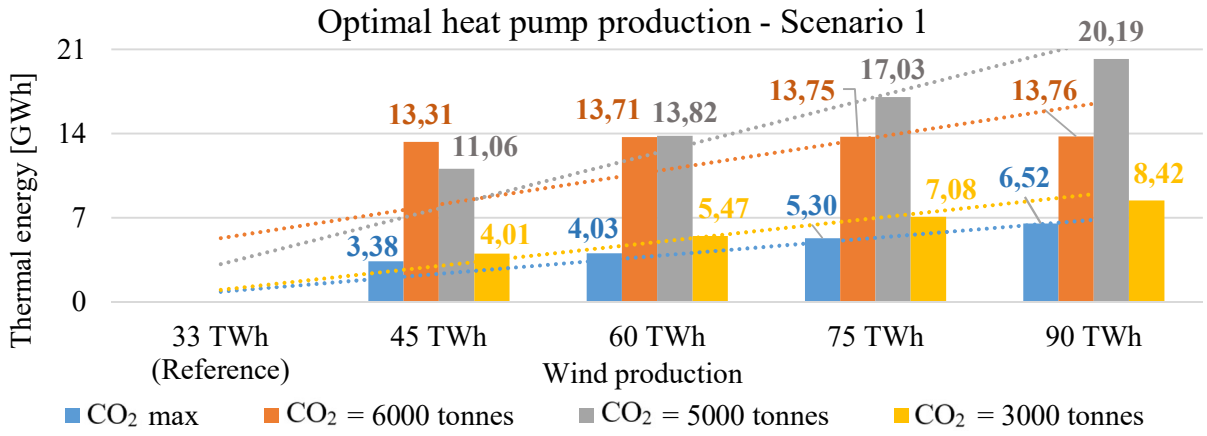

Figure 11 Optimal heat pump thermal energy production – Scenario 1

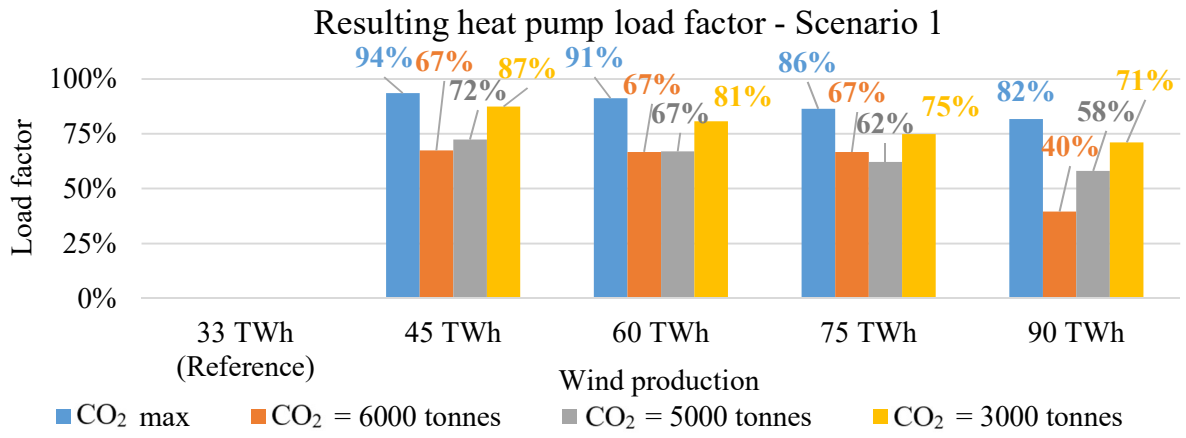

Figure 12 Resulting heat pump load factor – Scenario 1

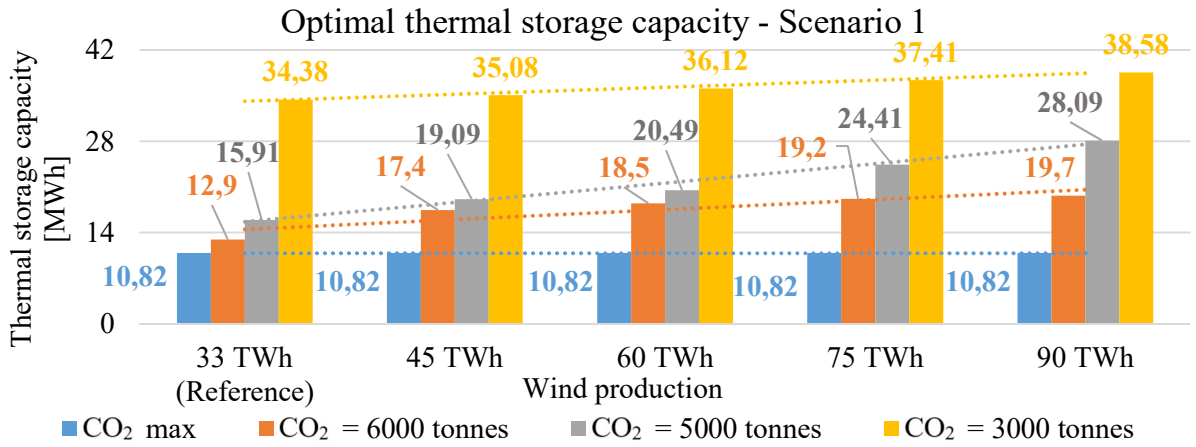

Figure 13 Optimal thermal storage capacity – Scenario 1

4.3. Optimal heat pump parameters – Scenario 2

Similarly to the analysis shown in Section 4.2 for Scenario 1, this section provides a detailed overview of the results for Scenario 2. In this scenario, the assumed power sector emission factor is equal to the ideal zero tonnes of CO_2/MWh. Figure 14 shows the Pareto front shift for Scenario 2. Similarly to Scenario 1, the Pareto fronts are also moving to the region of lower total costs and lower environmental impact. However, in this case the Pareto fronts are diverging when they approach the region of lower CO_2 emissions. The reason behind this is that the power sector emissions are equal to zero, which allows for the utilization of heat pumps, thus reducing the overall price and CO_2 emissions.

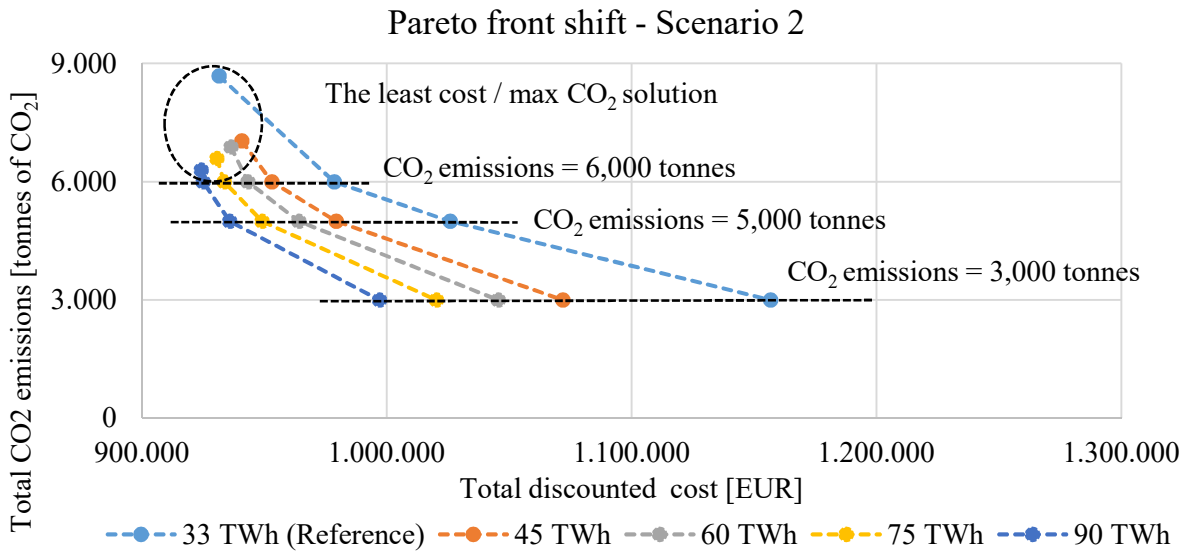

Figure 14 Pareto front shift for different wind penetration values – Scenario 2

Figure 15 shows the optimal heat pump capacities for Scenario 2. When compared with Scenario 1, this scenario also includes a heat pump as the optimal solution for the reference wind penetration of 33 TWh. Furthermore, the heat pump capacities increase as we approach the most environmentally friendly solution. The steepest trend is obtained for the least costly solution, which have the highest CO_2 emissions.

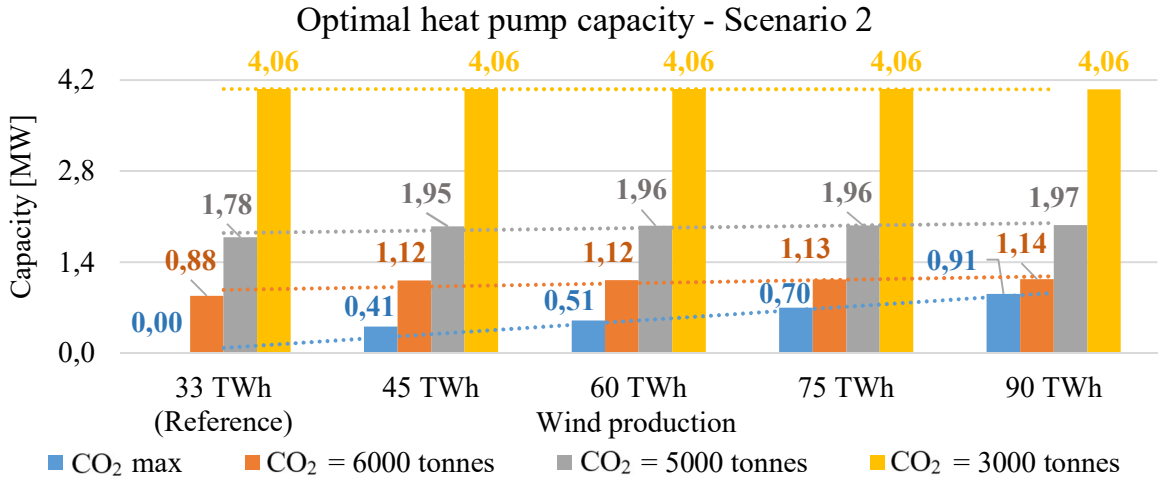

Figure 15 Optimal heat pump capacities – Scenario 2

Figure 16 shows the optimal heat pump production and has a similar trend as shown in Figure 12. As in Scenario 1, the load factor is also relatively high, around 0.6, as seen in Figure 17. Figure 18 shows the optimal thermal storage capacity for different wind energy penetration for Scenario 2. The steepest trend is acquired for the lowest observed CO_2 emissions, reaching up to 37 MWh.

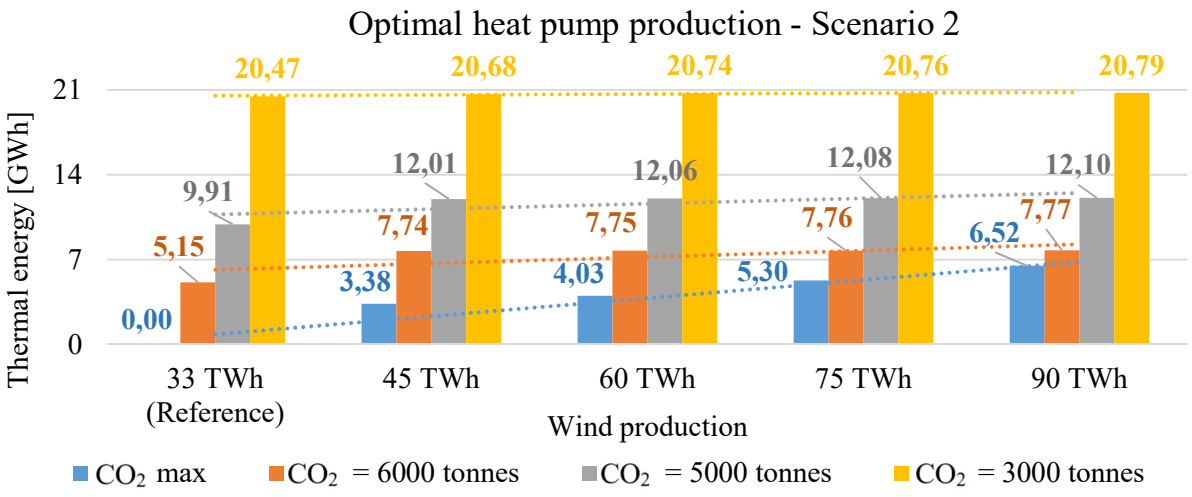

Figure 16 Optimal heat pump thermal energy production – Scenario 2

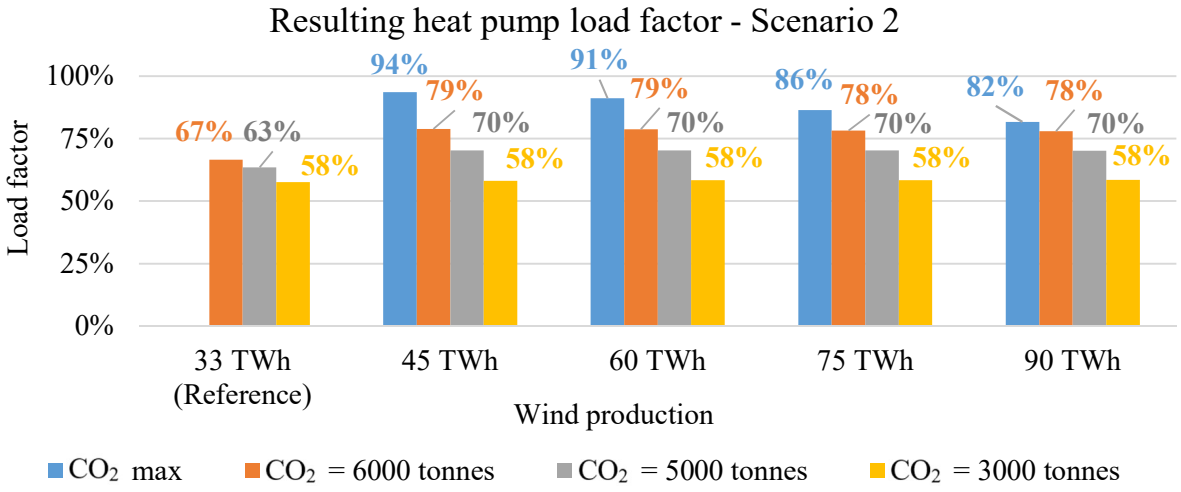

Figure 17 Resulting heat pump load factor - Scenario 2

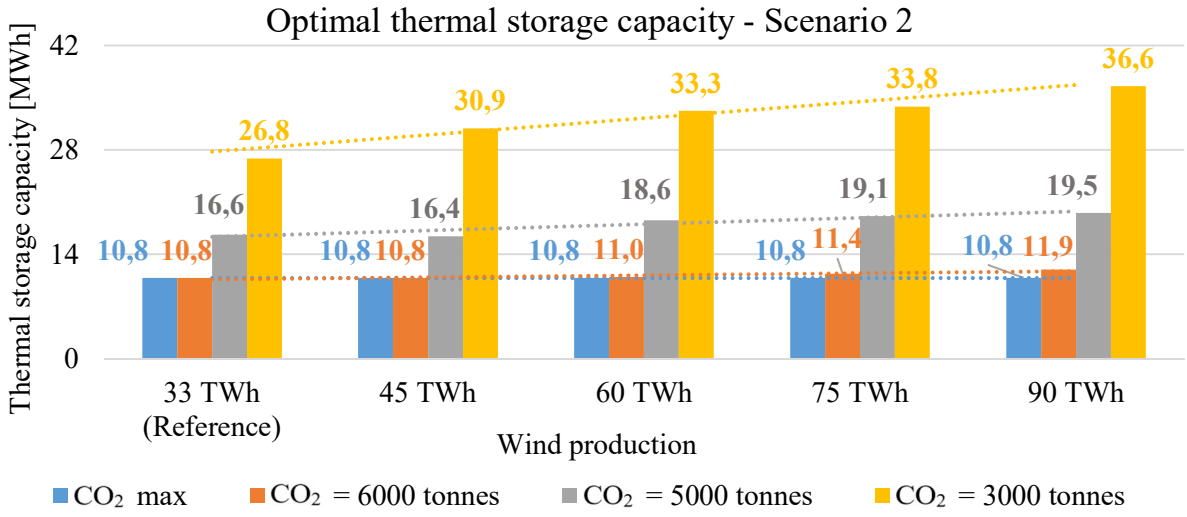

Figure 18 Optimal thermal storage capacity – Scenario 2

4.4. District heating system operation comparison

This section shows a detailed comparison of optimal district heating supply system operation for different levels of wind production penetration and CO_2 emissions. In order to analyse the impact of heating load seasonality, the hourly operation for winter and summer week is shown.

4.4.1. The least-cost/maximum CO_2 emissions solution

Figure 19 shows the DH system operation for a winter week of the least-cost solution for the wind penetration of 45 TWh and 60 TWh of wind. It can be seen that the heat pump operates in the same manner for both levels of wind energy penetration – at full load for a whole week, while charging the thermal storage during the night. The small difference can be seen when analysing the operation of the thermal storage. During night period, thermal storage is more charged for 60 TWh of wind penetration than with 45 TWh, due to the higher heat pump capacity and its utilization.

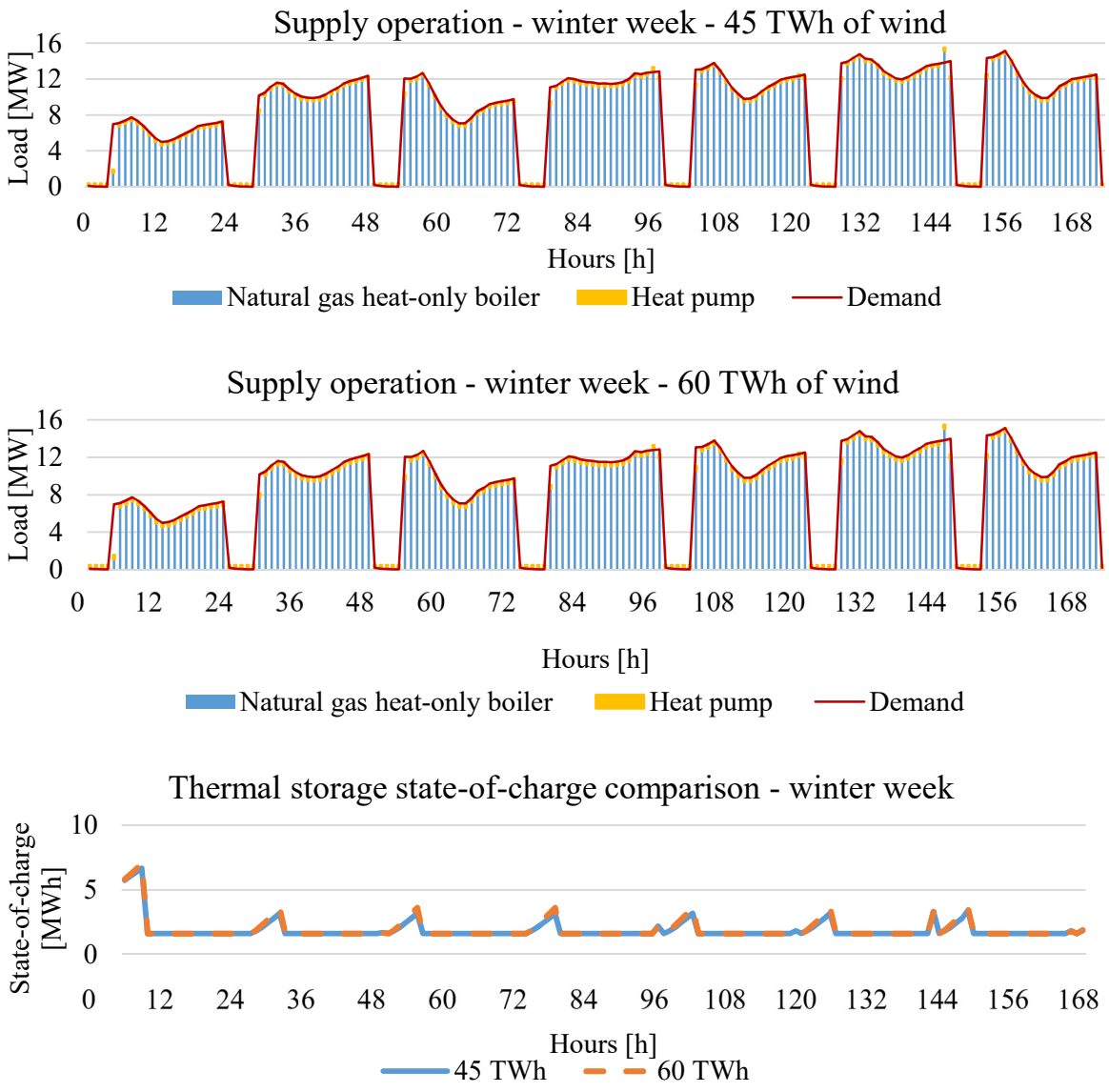

Figure 19 District heating system operation comparison for different levels of wind penetration for winter week – the least-cost solution

The difference in operation between the 45 TWh and the 60 TWh wind penetration is more obvious during summertime when the load is much smaller, only up to 1 MW. A smaller heat pump, obtained for lower wind penetration, can operate through the whole week, while a larger heat pump, obtained for higher wind penetration, will be much more dependent on the market price, i.e. during some hours, it will be able to shut down. Furthermore, the strategy of thermal storage charging is different when wind penetration is increased.

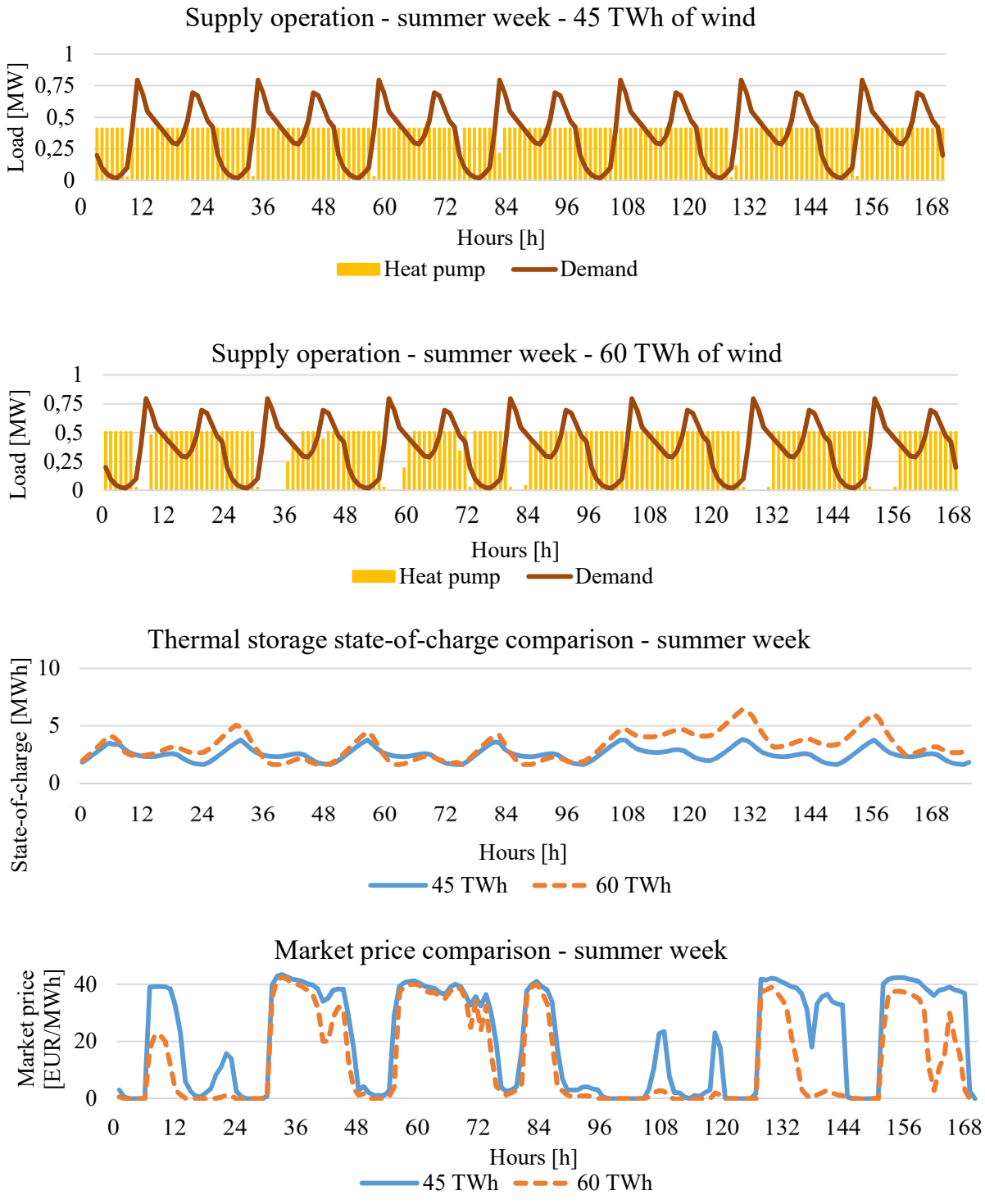

Figure 20 District heating system operation comparison for different levels of wind penetration for a summer week – the least-cost solution

4.4.2. Pareto optimal solution – 5,000 tonnes of CO_2 emissions solution

Figure 21 shows the optimal DH system operation for CO_2 emissions value of 5,000 tonnes. When compared to the least-cost solution it can be noted that a biomass boiler is also part of the optimal solution. Once again, the differences are not that obvious, but it can be seen that the state-of-charge of the thermal storage for 60 TWh of wind penetration is a little higher during the night period due to the higher optimal capacity of the heat pump.

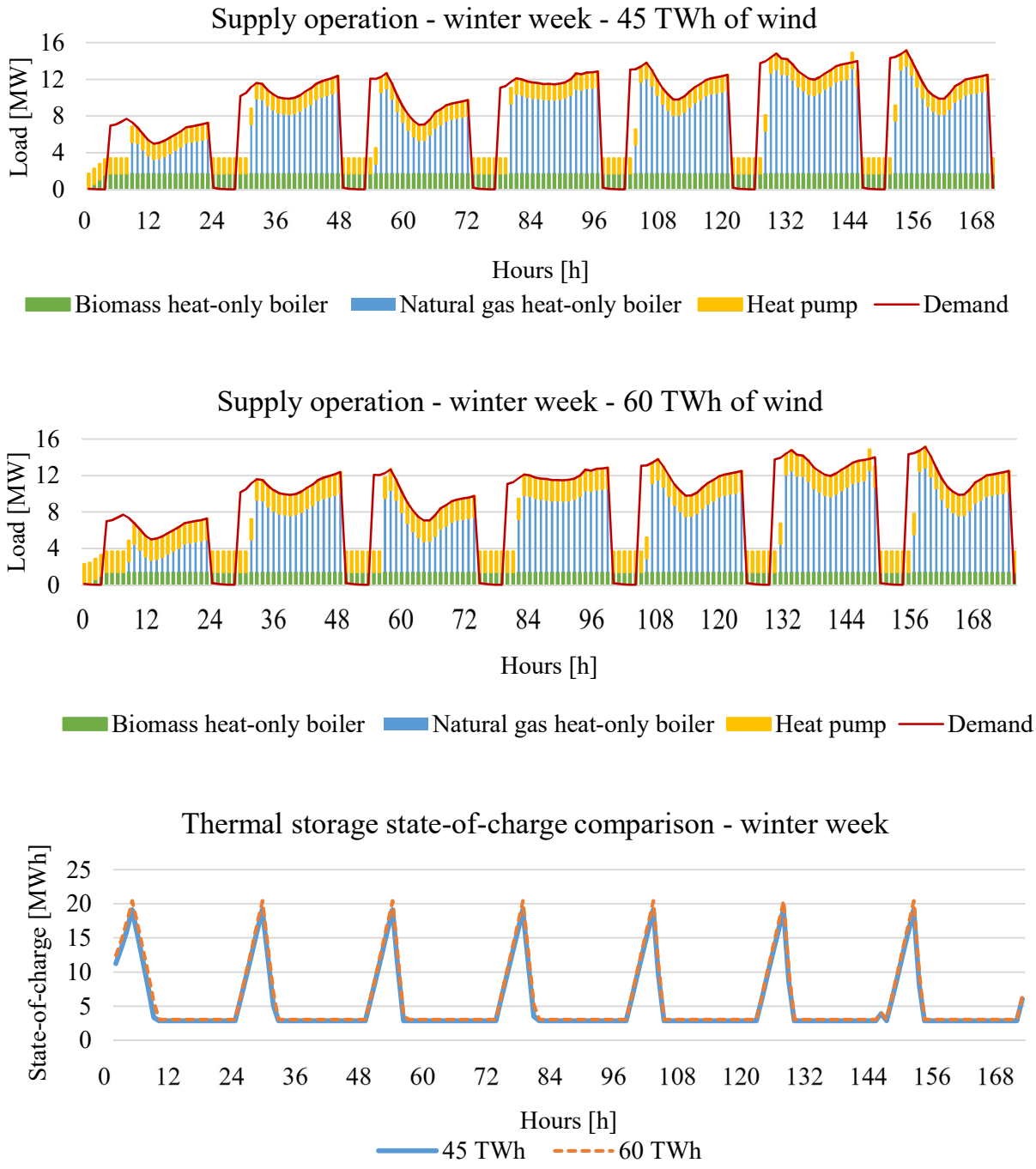

Figure 21 District heating system operation comparison for different levels of wind penetration for a winter week – the Pareto solution with 5,000 tonnes of CO_2 emissions

Figure 22 shows a comparison of DH system operation for the CO_2 emissions value of 5,000 tonnes for two different wind penetrations. The differences between operational strategies are more evident during the summertime than during a winter week. This could especially be seen in the thermal storage operation. For higher wind penetration the thermal storage is more utilized than for 45 TWh of wind production penetration.

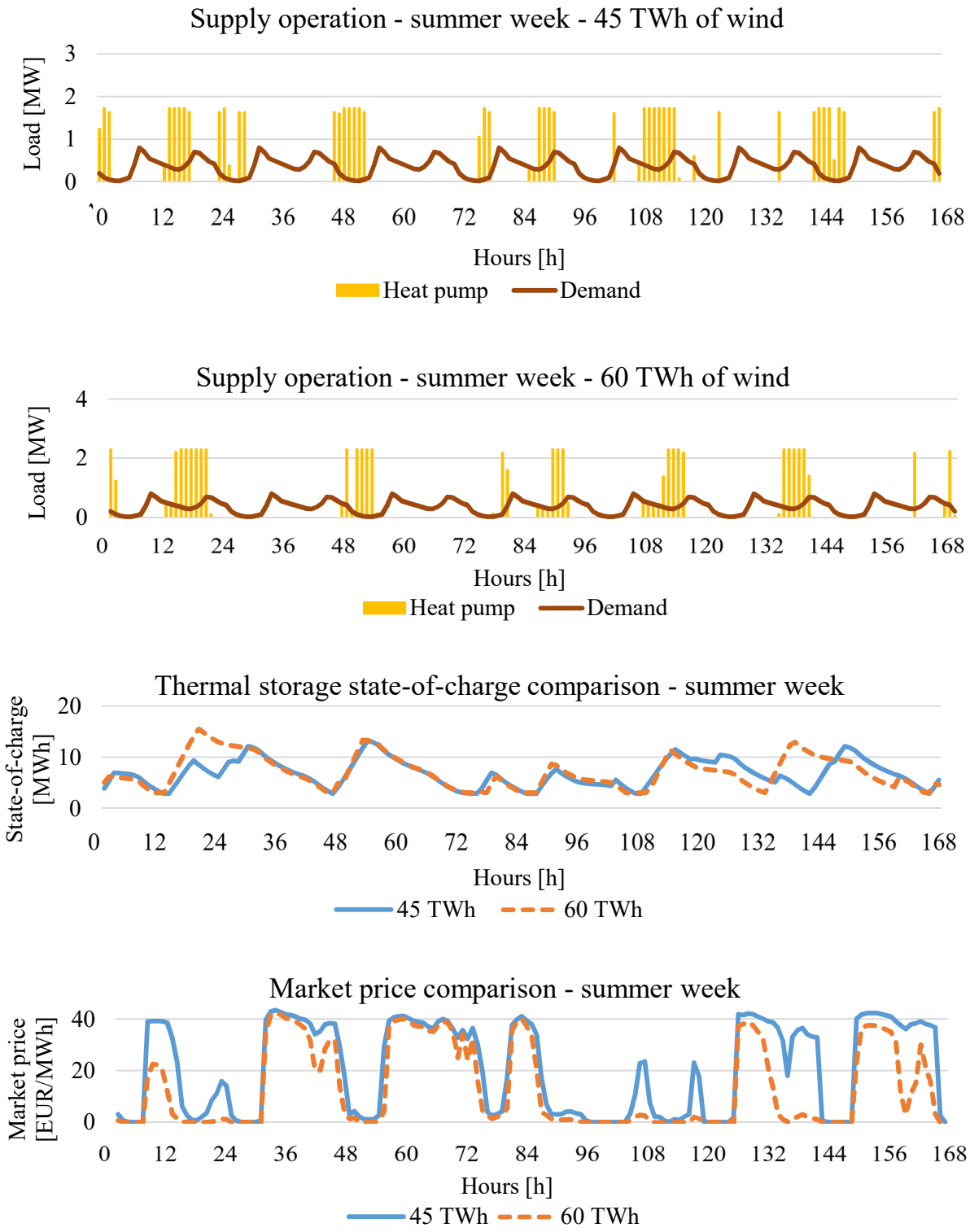

Figure 22 District heating system operation comparison for different levels of wind penetration for a summer week – the Pareto solution with 5,000 tonnes of CO_2 emissions

5. Conclusion

In this paper, an analysis of optimal heat pump capacities was performed with regard to the penetration of variable renewable energy sources. A multi-objective optimization model was used in order to acquire the optimal configuration of the district heating supply system and its operation. In order to evaluate the impact of wind production penetration on the optimal heat pump capacities, the electricity market clearing price was modelled by using publicly available Nord Pool market bidding data. The correlation between the increased wind energy production and the market price was obtained. Two scenarios were developed. In the first one, the power sector emission factor was equal to the historical one, while in the second scenario the power sector emission factor was reduced to zero. The obtained results show that increase of wind capacities enables higher capacities and thermal production of heat pumps. In Scenario 1, this was accomplished only for wind production higher than 33 TWh. However, in Scenario 2, heat pumps are part of the optimal solution for all studied electricity market prices. Furthermore, it was shown that the thermal storage capacity also increases with wind penetration.

Acknowledgements

Financial support from the RESFLEX project funded by the Programme of the Government of Republic of Croatia, Croatian Environmental Protection and Energy Efficiency Fund with the support of the Croatian Science Foundation for encouraging research and development activities in the area of Climate Change for the period from 2015 to 2016 in the amount of 1.344.100 HRK is gratefully acknowledged.

Appendix

A district heating model is shown in Figure A.1. The scheme visualizes different supply technology types and their interconnections, including short-term and long-term thermal energy storage. Furthermore, Figure A.1 displays the optimization variables: the supply capacities P_i, i.e. thermal storage size TES_{size}, and the hourly operation of the system Q_t, i.e. the thermal storage charge and discharge TES_{in-ou} . All technologies must cover the district heating demand DEM_t. Finally, the connection with the hourly electricity market can be noted. Power-to-heat technologies (heat pump and electrical heater) buy electricity and cogeneration units sell it on the hourly market. The hourly electricity market clearing price is marked with MCP_t.

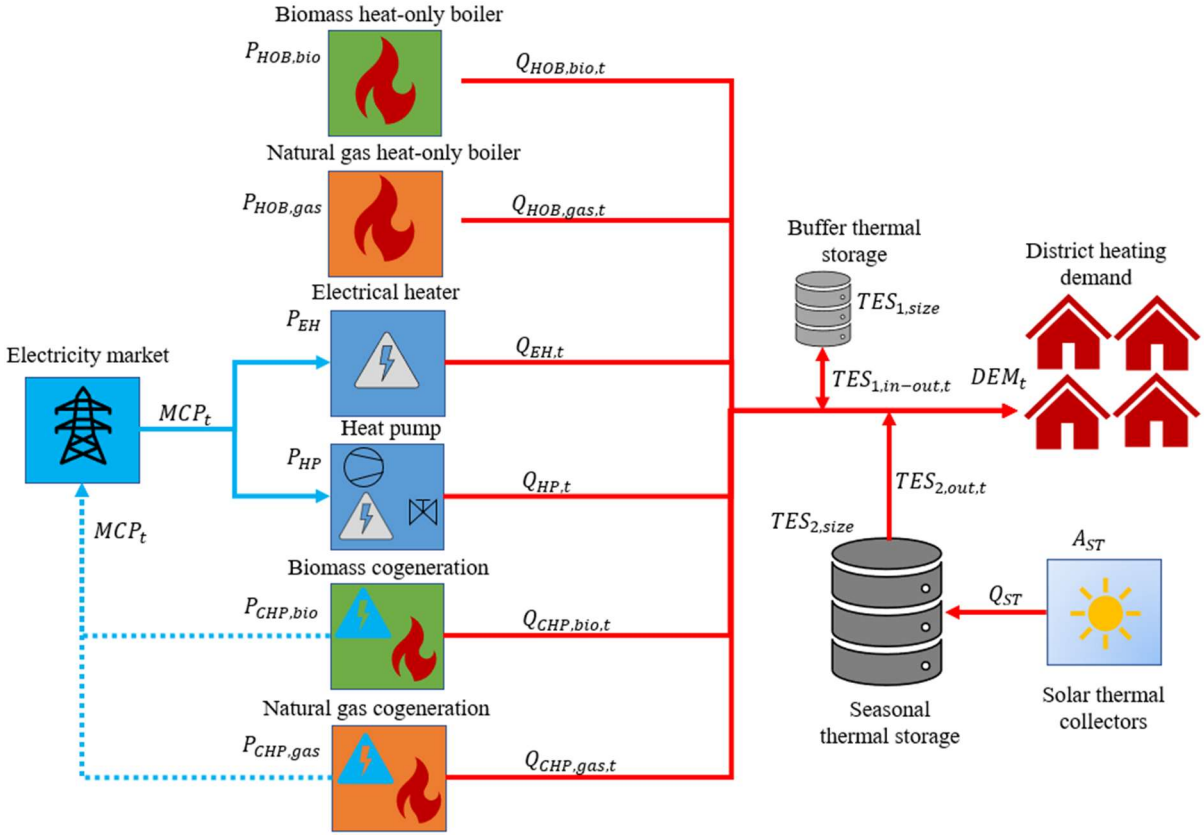

Figure A.1 District heating model

The district heating load used in this paper is shown in Figure A.1. It is constituted of the domestic hot water and space heating demand with a strong seasonal effect. The maximum demand is equal to 20 MW.

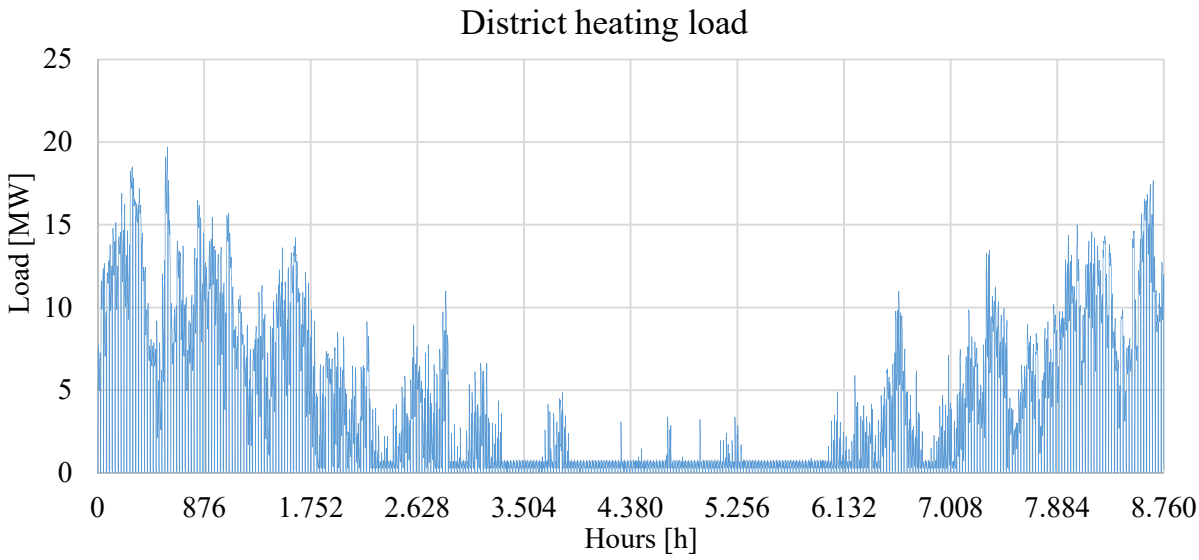

Figure A.2 District heating load

References

[1] A. R. Mazhar, S. Liu, and A. Shukla, "A state of art review on the district heating systems," *Renew. Sustain. Energy Rev.*, vol. 96, no. August, pp. 420–439, 2018, doi: 10.1016/j.rser.2018.08.005.

[2] A. Lake, B. Rezaie, and S. Beyerlein, "Review of district heating and cooling systems for a sustainable future," *Renew. Sustain. Energy Rev.*, vol. 67, pp. 417–425, 2017, doi: 10.1016/j.rser.2016.09.061.

[3] M. Wahlroos and M. Pärssinen, "Future views on waste heat utilization – Case of data centers in Northern Europe," *Renew. Sustain. Energy Rev.*, vol. 82, no. July 2017, pp. 1749–1764, 2018, doi: 10.1016/j.rser.2017.10.058.

[4] H. Lund, N. Duic, P. A. Ostergaard, and B. V. Mathiesen, "Future District Heating Systems and Technologies : On the role of Smart Energy Systems and 4 th Generation District," *Energy*, 2018, doi: 10.1016/j.energy.2018.09.115.

[5] H. Lund *et al.*, "4th Generation District Heating (4GDH). Integrating smart thermal grids into future sustainable energy systems.," *Energy*, vol. 68, pp. 1–11, 2014, doi: 10.1016/j.energy.2014.02.089.

[6] H. Lund, B. Möller, B. V. Mathiesen, and A. Dyrelund, "The role of district heating in future renewable energy systems," *Energy*, vol. 35, no. 3, pp. 1381–1390, 2010, doi: 10.1016/j.energy.2009.11.023.

[7] D. Olsthoorn, F. Haghighat, and P. A. Mirzaei, "Integration of storage and renewable energy into district heating systems: A review of modelling and optimization," *Sol. Energy*, vol. 136, pp. 49–64, 2016, doi: 10.1016/j.solener.2016.06.054.

[8] P. A. Østergaard, "Reviewing EnergyPLAN simulations and performance indicator applications in EnergyPLAN simulations," *Applied Energy*, vol. 154. pp. 921–933, 2015, doi: 10.1016/j.apenergy.2015.05.086.

[9] P. A. Østergaard and A. N. Andersen, "Booster heat pumps and central heat pumps in district heating," *Appl. Energy*, vol. 184, pp. 1374–1388, 2016, doi: 10.1016/j.apenergy.2016.02.144.

[10] R. Mikulandrić *et al.*, "Performance analysis of a hybrid district heating system: A case study of a small town in Croatia," *J. Sustain. Dev. Energy, Water Environ. Syst.*, vol. 3, no. 3, pp. 282–302, 2015, doi: 10.13044/j.sdewes.2015.03.0022.

[11] P. Prebeg, G. Gasparovic, G. Krajacic, and N. Duic, "Long-term energy planning of Croatian power system using multi-objective optimization with focus on renewable energy and integration of electric vehicles," *Appl. Energy*, 2016, doi: 10.1016/j.apenergy.2016.03.086.

[12] M. A. Sayegh *et al.*, "Trends of European research and development in district heating technologies," *Renew. Sustain. Energy Rev.*, vol. 68, pp. 1183–1192, 2017, doi: 10.1016/j.rser.2016.02.023.

[13] H. Ahvenniemi and K. Klobut, "Future services for district heating solutions in residential districts," *J. Sustain. Dev. Energy, Water Environ. Syst.*, vol. 2, no. 2, pp. 127–138, 2014, doi: 10.13044/j.sdewes.2014.02.0012.

[14] S. Buffa, M. Cozzini, M. D'Antoni, M. Baratieri, and R. Fedrizzi, "5th generation

district heating and cooling systems: A review of existing cases in Europe," *Renew. Sustain. Energy Rev.*, vol. 104, no. June 2018, pp. 504–522, 2019, doi: 10.1016/j.rser.2018.12.059.

[15] A. Arabkoohsar and A. S. Alsagri, "Thermodynamic analysis of ultralow-temperature district heating system with shared power heat pumps and triple-pipes," *Energy*, vol. 194, p. 116918, 2020, doi: 10.1016/j.energy.2020.116918.

[16] M. Tańczuk, J. Skorek, and P. Bargiel, "Energy and economic optimization of the repowering of coal-fired municipal district heating source by a gas turbine," *Energy Convers. Manag.*, vol. 149, pp. 885–895, 2017, doi: 10.1016/j.enconman.2017.03.053.

[17] A. Niromandfam, A. S. Yazdankhah, and R. Kazemzadeh, "Modeling Demand Response based on Utility function considering wind profit maximization in the day-ahead market," *J. Clean. Prod.*, 2019, doi: 10.1016/j.jclepro.2019.119317.

[18] G. Li and J. Shi, "Agent-based modeling for trading wind power with uncertainty in the day-ahead wholesale electricity markets of single-sided auctions," *Appl. Energy*, vol. 99, pp. 13–22, 2012, doi: 10.1016/j.apenergy.2012.04.022.

[19] L. Chinmoy, S. Iniyan, and R. Goic, "Modeling wind power investments, policies and social benefits for deregulated electricity market – A review," *Appl. Energy*, vol. 242, no. May 2018, pp. 364–377, 2019, doi: 10.1016/j.apenergy.2019.03.088.

[20] S. S. Reddy, P. R. Bijwe, and A. R. Abhyankar, "Electrical Power and Energy Systems Optimum day-ahead clearing of energy and reserve markets with wind power generation using anticipated real-time adjustment costs," *Int. J. Electr. Power Energy Syst.*, vol. 71, pp. 242–253, 2015, doi: 10.1016/j.ijepes.2015.03.002.

[21] M. Doostizadeh, F. Aminifar, H. Lesani, and H. Ghasemi, "Multi-area market clearing in wind-integrated interconnected power systems: A fast parallel decentralized method," *Energy Convers. Manag.*, vol. 113, pp. 131–142, 2016, doi: 10.1016/j.enconman.2016.01.047.

[22] S. Fogelberg and E. Lazarczyk, "Wind power volatility and its impact on production failures in the Nordic electricity market," *Renew. Energy*, vol. 105, pp. 96–105, 2017, doi: 10.1016/j.renene.2016.12.024.

[23] R. P. Odeh and D. Watts, "Impacts of wind and solar spatial diversification on its market value : A case study of the Chilean electricity market," *Renew. Sustain. Energy Rev.*, vol. 111, no. May, pp. 442–461, 2019, doi: 10.1016/j.rser.2019.01.015.

[24] F. Isaza and S. Botero, "Wind power reliability valuation in a Hydro-Dominated power market : The Colombian case," *Renew. Sustain. Energy Rev.*, vol. 57, pp. 1359–1372, 2016, doi: 10.1016/j.rser.2015.12.159.

[25] M. Pavičević, T. Novosel, T. Pukšec, and N. Duić, "Hourly optimization and sizing of district heating systems considering building refurbishment - Case study for the city of Zagreb," *Energy*, 2016, doi: 10.1016/j.energy.2017.06.105.

[26] J. P. Jiménez Navarro, J. M. Cejudo López, and D. Connolly, "The effect of feed-in-tariff supporting schemes on the viability of a district heating and cooling production system," *Energy*, vol. 134, pp. 438–448, 2017, doi: 10.1016/j.energy.2017.05.174.

[27] T. Falke, S. Krengel, A.-K. Meinerzhagen, and A. Schnettler, "Multi-objective optimization and simulation model for the design of distributed energy systems," *Appl.*

Energy, 2016, doi: 10.1016/j.apenergy.2016.03.044.

[28] D. Wei, A. Chen, B. Sun, and C. Zhang, "Multi-objective optimal operation and energy coupling analysis of combined cooling and heating system," *Energy*, vol. 98, pp. 296–307, 2016, doi: 10.1016/j.energy.2016.01.027.

[29] M. Pirouti, A. Bagdanavicius, J. Ekanayake, J. Wu, and N. Jenkins, "Energy consumption and economic analyses of a district heating network," *Energy*, vol. 57, pp. 149–159, 2013, doi: 10.1016/j.energy.2013.01.065.

[30] N. Lamaison, S. Collette, M. Vallée, and R. Bavière, "Storage influence in a combined biomass and power-to-heat district heating production plant," *Energy*, vol. 186, 2019, doi: 10.1016/j.energy.2019.07.044.

[31] M. Åberg, L. Fälting, D. Lingfors, A. M. Nilsson, and A. Forssell, "Do ground source heat pumps challenge the dominant position of district heating in the Swedish heating market?," *J. Clean. Prod.*, vol. 254, 2020, doi: 10.1016/j.jclepro.2020.120070.

[32] K. Kontu, S. Rinne, and S. Junnila, "Introducing modern heat pumps to existing district heating systems – Global lessons from viable decarbonizing of district heating in Finland," *Energy*, vol. 166, pp. 862–870, 2019, doi: 10.1016/j.energy.2018.10.077.

[33] P. Sorknæs, S. R. Djørup, H. Lund, and J. Z. Thellufsen, "Quantifying the influence of wind power and photovoltaic on future electricity market prices," *Energy Convers. Manag.*, vol. 180, no. November 2018, pp. 312–324, 2019, doi: 10.1016/j.enconman.2018.11.007.

[34] S. Amiri and G. Weinberger, "Increased cogeneration of renewable electricity through energy cooperation in a Swedish district heating system - A case study," *Renew. Energy*, vol. 116, pp. 866–877, 2018, doi: 10.1016/j.renene.2017.10.003.

[35] S. Djørup, J. Z. Thellufsen, and P. Sorknæs, "The electricity market in a renewable energy system," *Energy*, 2018, doi: 10.1016/j.energy.2018.07.100.

[36] B. Felten, "An integrated model of coupled heat and power sectors for large-scale energy system analyses," *Appl. Energy*, vol. 266, no. January, p. 114521, 2020, doi: 10.1016/j.apenergy.2020.114521.

[37] S. Mosquera-lópez and A. Nursimulu, "Drivers of electricity price dynamics : Comparative analysis of spot and futures markets," *Energy Policy*, vol. 126, no. November 2018, pp. 76–87, 2019, doi: 10.1016/j.enpol.2018.11.020.

[38] W. Liu, D. Klip, W. Zappa, S. Jelles, and G. Jan, "The marginal-cost pricing for a competitive wholesale district heating market: A case study in the Netherlands," *Energy*, no. 189, p. 116367, 2019, doi: 10.1016/j.energy.2019.116367.

[39] J. Hennessy, H. Li, F. Wallin, and E. Thorin, "Towards smart thermal grids : Techno-economic feasibility of commercial heat-to-power technologies for district heating," *Appl. Energy*, vol. 228, no. June, pp. 766–776, 2018, doi: 10.1016/j.apenergy.2018.06.105.

[40] D. Wang *et al.*, "Integrated demand response in district electricity-heating network considering double auction retail energy market based on demand-side energy stations," *Appl. Energy*, vol. 248, no. January, pp. 656–678, 2019, doi: 10.1016/j.apenergy.2019.04.050.

[41] Z. Yifan *et al.*, "Power and Energy Flexibility of District Heating System and Its Application in Wide-Area Power and Heat Dispatch," *Energy*, p. 116426, 2019, doi: 10.1016/j.energy.2019.116426.

[42] J. Wang, Z. Zhou, J. Zhao, J. Zheng, and Z. Guan, "Optimizing for clean-heating improvements in a district energy system with high penetration of wind power," *Energy*, vol. 175, pp. 1085–1099, 2019, doi: 10.1016/j.energy.2019.03.153.

[43] F. Levihn, "CHP and heat pumps to balance renewable power production: Lessons from the district heating network in Stockholm," *Energy*, vol. 137, pp. 670–678, 2017, doi: 10.1016/j.energy.2017.01.118.

[44] S. Moser, S. Puschnigg, and V. Rodin, "Designing the Heat Merit Order to determine the value of industrial waste heat for district heating systems," *Energy*, vol. 200, p. 117579, 2020, doi: 10.1016/j.energy.2020.117579.

[45] J. Wang, S. You, Y. Zong, H. Cai, C. Træholt, and Z. Y. Dong, "Investigation of real-time flexibility of combined heat and power plants in district heating applications," *Appl. Energy*, vol. 237, no. November 2018, pp. 196–209, 2019, doi: 10.1016/j.apenergy.2019.01.017.

[46] D. Lingfors, J. Olauson, D. Lingfors, and J. Olauson, "Can electricity market prices control power-to-heat production for peak shaving of renewable power generation ? The case of Sweden," *Energy*, vol. 176, no. 1, pp. 1–14, 2019, doi: 10.1016/j.energy.2019.03.156.

[47] O. Terreros *et al.*, "Electricity market options for heat pumps in rural district heating networks in Austria," *Energy*, vol. 196, p. 116875, 2020, doi: 10.1016/j.energy.2019.116875.

[48] P. A. Østergaard, J. Jantzen, H. M. Marczinkowski, and M. Kristensen, "Business and socioeconomic assessment of introducing heat pumps with heat storage in small-scale district heating systems," *Renew. Energy*, vol. 139, pp. 904–914, 2019, doi: 10.1016/j.renene.2019.02.140.

[49] D. Böttger, M. Götz, M. Theofilidi, and T. Bruckner, "Control power provision with power-to-heat plants in systems with high shares of renewable energy sources - An illustrative analysis for Germany based on the use of electric boilers in district heating grids," *Energy*, vol. 82, pp. 157–167, 2015, doi: 10.1016/j.energy.2015.01.022.

[50] M. Ito, A. Takano, T. Shinji, T. Yagi, and Y. Hayashi, "Electricity adjustment for capacity market auction by a district heating and cooling system," *Appl. Energy*, vol. 206, no. August, pp. 623–633, 2017, doi: 10.1016/j.apenergy.2017.08.210.

[51] J. Zheng, Z. Zhou, J. Zhao, and J. Wang, "Effects of the operation regulation modes of district heating system on an integrated heat and power dispatch system for wind power integration," *Appl. Energy*, vol. 230, no. September, pp. 1126–1139, 2018, doi: 10.1016/j.apenergy.2018.09.077.

[52] A. Gravelsins, I. Pakere, A. Tukulis, and D. Blumberga, "Solar power in district heating. P2H flexibility concept," *Energy*, vol. 181, pp. 1023–1035, 2019, doi: 10.1016/j.energy.2019.05.224.

[53] B. Leitner, E. Widl, W. Gawlik, and R. Hofmann, "A method for technical assessment of power-to-heat use cases to couple local district heating and electrical distribution

grids," *Energy*, vol. 182, pp. 729–738, 2019, doi: 10.1016/j.energy.2019.06.016.

[54] D. F. Dominković, M. Wahlroos, S. Syri, and A. S. Pedersen, "Influence of different technologies on dynamic pricing in district heating systems: Comparative case studies," *Energy*, vol. 153, no. March, pp. 136–148, 2018, doi: 10.1016/j.energy.2018.04.028.

[55] E. Sandberg, J. G. Kirkerud, E. Trømborg, and T. F. Bolkesjø, "Energy system impacts of grid tariff structures for flexible power-to-district heat," *Energy*, vol. 168, pp. 772–781, 2019, doi: 10.1016/j.energy.2018.11.035.

[56] H. Averfalk, P. Ingvarsson, U. Persson, M. Gong, and S. Werner, "Large heat pumps in Swedish district heating systems," *Renew. Sustain. Energy Rev.*, vol. 79, no. May, pp. 1275–1284, 2017, doi: 10.1016/j.rser.2017.05.135.

[57] P. A. Østergaard and A. N. Andersen, "Economic feasibility of booster heat pumps in heat pump-based district heating systems," *Energy*, 2018, doi: 10.1016/j.energy.2018.05.076.

[58] K. Askeland, K. N. Bozhkova, and P. Sorknæs, "Balancing Europe : Can district heating affect the flexibility potential of Norwegian hydropower resources ?," *Renew. Energy*, vol. 141, no. 2019, pp. 646–656, 2020, doi: 10.1016/j.renene.2019.03.137.

[59] M. Swing, J. Are, and E. Dotzauer, "Potential for district heating to lower peak electricity demand in a medium-size municipality in Sweden," *J. Clean. Prod.*, vol. 186, pp. 1–9, 2018, doi: 10.1016/j.jclepro.2018.03.038.

[60] P. Sorknæs *et al.*, "Smart Energy Markets - Future electricity, gas and heating markets," *Renew. Sustain. Energy Rev.*, vol. 119, no. March 2019, 2020, doi: 10.1016/j.rser.2019.109655.

[61] M. A. Mirzaei *et al.*, "Evaluating the impact of multi-carrier energy storage systems in optimal operation of integrated electricity, gas and district heating networks," *Appl. Therm. Eng.*, vol. 176, p. 115413, 2020, doi: 10.1016/j.applthermaleng.2020.115413.

[62] J. Jimenez-Navarro, K. Kavvadias, F. Filippidou, M. Pavičević, and S. Quoilin, "Coupling the heating and power sectors : The role of centralised combined heat and power plants and district heat in a European decarbonised power system," *Appl. Energy*, vol. 270, no. May, 2020, doi: 10.1016/j.apenergy.2020.115134.

[63] H. Dorotić, T. Pukšec, and N. Duić, "Multi-objective optimization of district heating and cooling systems for a one-year time horizon," *Energy*, 2019, doi: 10.1016/j.energy.2018.11.149.

[64] H. Dorotić, T. Pukšec, and N. Duić, "Economical, environmental and exergetic multi-objective optimization of district heating systems on hourly level for a whole year," *Appl. Energy*, vol. 251, p. 113394, Oct. 2019, doi: 10.1016/j.apenergy.2019.113394.

[65] JRC, "PVGIS." [Online]. Available: http://re.jrc.ec.europa.eu/pvgis.html, the last access 28/06/2020

[66] "Renewable ninja." [Online]. Available: https://www.renewables.ninja/, the last access 28/06/2020

[67] P. A. Sørensen, J. E. Nielsen, R. Battisti, T. Schmidt, and D. Trier, "Solar district heating guidelines: Collection of fact sheets," no. August, p. 152, 2012.

[68] “SPF Institut für Solartechnik.” [Online]. Available: http://www.spf.ch/index.php?id=111&L=6, the last access 28/06/2020

[69] S. Frederiksen and S. Werner, *District Heating and Cooling*. 2013.

[70] W. Jakob and C. Blume, “Pareto optimization or cascaded weighted sum: A comparison of concepts,” *Algorithms*, vol. 7, no. 1, pp. 166–185, 2014, doi: 10.3390/a7010166.

[71] M. Dillig, M. Jung, and J. Karl, “The impact of renewables on electricity prices in Germany – An estimation based on historic spot prices in the years 2011 – 2013,” *Renew. Sustain. Energy Rev.*, vol. 57, pp. 7–15, 2016, doi: 10.1016/j.rser.2015.12.003.

[72] “Nord Pool.”

[73] K. Van Den Bergh and E. Delarue, “Cycling of conventional power plants: Technical limits and actual costs,” *Energy Convers. Manag.*, vol. 97, pp. 70–77, 2015, doi: 10.1016/j.enconman.2015.03.026.

[74] “Danish Energy Agency, Technology database.” .